

# Modelling Ordering Phenomena in Substitutional Binary Alloys Using a Spin-1 Ising Model

Diego Alejandro Herrera Rojas

September 2020

## Abstract

Order-disorder phase transitions in 2D binary substitutional alloys  $A_xB_{1-x}$ , following the prototype of  $\beta$ -brass, are studied. By means of a spin-1 Ising model in a centered rectangular lattice, the effect of finite vacancy concentration,  $y$ , is examined in the context of the grand canonical potential, using chemical potentials  $\zeta$  and  $\nu$  as parameters. The critical curve of second order transitions in the planes  $x-T$  and  $\zeta-T$  is studied from a mean field approximation, in the context of the grand canonical ensemble. A closed expression for the critical curve in  $x-T$  plane is derived. The curves obtained in  $\zeta-T$  plane will be compared to Monte Carlo calculations following Glauber dynamics. Numerical calculations in the limit of zero vacancy concentration are compared to the spin-1/2 Ising Model class, which is the most commonly used model for studying second order transitions in binary alloys, so as to characterise the influence of vacancy concentration in ordering phase transitions.

# Nomenclature

## Mathematical Convention

$\delta_{i,\nu}^{(X)}$  Kroenecker delta on  $S_i^{(X)}$ , defined on a lattice site  $i$  of sublattice  $X$ .

$\sum_{\langle i_{A_2}, j_{B_2} \rangle}$  Sumation over nearest neigbours on bipartite sublattice.

$\sum_{i_X}$  Summation over all lattice sites on sublattice  $X$  of a lattice.

## Heuristic Constants

$\epsilon_{XY}$  Bond energy between particle types  $X$  and  $Y$

$N_{XY}$  Number of nearest neighbour bonds between particles of type  $X$  and  $Y$

## Lattice Parameters

$A_2, B_2$  Sublattices of a bipartite sublattice.

$N$  Number of lattice sites.

$z$  Lattice coordination number.

## Hamiltonian Parameters

$h$  External magnetic field.

$J$  Exchange Integral in Ising-like Models.

$K$  Quadrupole interaction constant.

$S_i^{(X)}, S_{i_X}$  Spin-like lattice variable defined on sublattice  $X$  of a lattice.

$S_i$  Spin-like lattice variables.

## Thermodynamic Parameters

$\beta$  Inverse temperature.

$\mu$  Chemical potential difference between vacant lattice sites and atoms.

$\mu_X$  Chemical potential associated to  $X$  type particles.

$\zeta$  Chemical potential difference between atoms of different type.

$k_B$  Boltzman constant.

$N_X$  Number of  $X$  type particles in the system.

$x$  Concentration of  $A$  type atoms.

$y$  Concentration of vacant lattice sites.

# 1 Introduction

Phase transitions is one of the most important topics of research on statistical physics nowadays. Specifically, phase transitions of the second kind are of high interest due to their fascinating properties such as symmetry breaking or continuous state change [17]. Although exact analytical treatment of critical phenomena is quite complicated, a simple, yet powerful, model was developed by Ising in 1925, which emulated ferromagnetic (antiferromagnetic) transitions of some solids when cooled below a so called critical temperature. At first glance, the simplicity of the model is deceptive. Nevertheless, as pointed out in [12], the Ising model illustrates beautifully not only the most standard theoretical predictions from Ginzburg-Landau theory, but also how correlation between different components of a macroscopic system lead to critical phenomena.

The Ising Model has been successfully used in describing critical phenomena apart from magnetic solids. In [22], the Ising Model dynamics is applied to the order-disorder transition of a binary alloy ( $A_yB_{1-y}$ ) with a BCC structure. Due to restrictions on the number of particles of different species, the analysis in [22] was carried out in the context of the grand canonical ensemble. Phase diagrams were obtained, and the importance of the concentration of atoms ( $y$ ) was stressed. However, some features like vacancy-assisted diffusion or beyond nearest neighbour interaction were not considered [22].

Both in [22] and [12], generalisations of the Ising model are proposed as alternatives for modelling critical phenomena. The Blume-Emery-Griffiths (BEG) Model for studying  $\text{He}^3 - \text{He}^4$  mixtures has been used successfully to describe phase transitions in fluids, including vacancies or holes in the modelling lattice [4, 24]. From a computational point of view, in [22] is suggested that simulations using Kawasaki dynamics (in Monte Carlo Simulations) could be implemented in order to avoid studying binary alloys via grand canonical ensemble. Successful applications of this dynamics for modelling the former system can be found in [3]. However, in [3], the standard Ising Model was used to describe the phase transition and ordering.

Following the spirit of [22] and [4], the study of phase transitions will be performed mainly on the  $x - T$  and  $\zeta - T$  projections of the phase space. This analysis will be developed in the context of the grand canonical ensemble. Hence, by careful study of thermodynamic quantities that show special behaviour at transition points (i. e. specific heat, order parameters, internal energy) for given atom chemical potential difference  $\zeta$ , numerical and analytical estimation of critical curves in the mentioned phase space projection will be obtained and compared to those in [22] to determine the influence of vacancies in the ordering of the alloy. Vacancy concentration will be included as a fixed parameter in the model. A mean field approximation will be used to determine the general shape of critical curves. Monte Carlo simulations will be performed in order to establish better estimates of the critical curves in the  $\zeta - T$  plane.

In section 2, the concepts mentioned above are introduced in more detail, emphasising the importance of the correlation function and the relation between the Ising model and phase transitions in binary alloys. In section 4, the particular details of the aim of the project are exposed thoroughly, highlighting the analytical and numerical procedures that are to be performed. In section 6, the general and specific objectives of the project are introduced, highlighting how the project extends the work carried out in [12] and [22]. Modelling of a substitutional binary alloy using a Spin-1 Model allows not only to account for the influence of lattice phenomena on ordering transitions, but also constitutes a first step in studying the influence of doping and impurities on this type of phase transitions [19]. This would generalise commonly used Spin-1/2 models, such as that treated by Porta and Castán [22], and apply the standard techniques stated in Ibarra's work [12] to a non

magnetic system. In section 7, the methodology is introduced, carefully exposing details concerning analytical calculation of thermodynamic quantities in the mean field approximation and via Monte Carlo simulations. In section 9 a schedule is proposed in terms of relative times. In section 10, all available resources are listed and presented in terms of their function in the successful development of the project.

## 2 Theoretical Framework

The theoretical references for this project are [22] and [12]. On the **frist** subsection, the fundamental ideas concerning order-disorder transition in alloys are discussed. Following [22], the prototype for the physical system is  $\beta$ -brass ( $\text{CuZn}$ ) near stoichiometric concentrations 1 : 1. After presenting the nature of the ordering process in this type of alloys and the main mechanisms involved in atomic reorganisation, a simple yet powerful interaction Hamiltonian is derived. Explicit demonstration of the equivalence between a binary alloy similar to  $\beta$ -brass near an ordering phase transition and the 3D antiferromagnetic Ising Model is presented. On the **second** subsection, the statistical study of the Ising model is developed, following the insights of [12]. This is paramount to the statistical study of a binary alloy as will be demonstrated. The fundamental notions of Landau theory presented in [12] are introduced, and expanded upon [17]. Emphasis is placed upon the concept of critical exponents and the important tool of mean field approximations. The most important results concerning the study of the Ising Model are presented as in [12]. It is explicitly shown that the analysis of a binary alloy in the grand canonical ensemble can be performed by an almost direct extrapolation of the results obtained for the antiferromagnetic Ising Model. On the **third** section, a more general model for ordering transitions in alloys is presented. Te importance of vacant lattice sites is justified by considering the nature of diffusion in solid metallic solutions. Since this motivates the definition of a spin-1 lattice variable, the Blume-Emery-Griffiths (BEG) model is discussed. The general definition of the BEG model is introduced from [4], emphasising on some of the nuances of the phase transitions in this particular model. Phase diagrams from [4] and [24] are presented as a tool for studying the nature of phase transitions. On section **last**, since the aim of the project demands a thorough study of the dynamics of the transition, fundamentals of Monte Carlo simulations are introduced. From [12], the celebrated Metropolis-Hastings algorithm is introduced. Furthermore, algorithms for computing thermodynamical quantities of interest are presented. More details on the subject of Monte Carlo simulations are included from [15].

### 2.1 Order-disorder transitions in $\beta$ -brass type alloys

Brass is a type of alloy composed by Cu and Zn. For low concentrations of Zn, the lattice structure of the solid is FCC, as in the pure solid form of Cu. However, near stoichiometric proportions 1 : 1, the lattice structure is BCC [6]. At high temperatures, all lattice points are indistinguishable in that the probability that an atom of Cu occupies a site is equal to the probability that it be occupied by an atom of Zn. However, when the system is at temperatures bellow a critical one ( $T_c \approx 733\text{K}$ ), atoms of each species tend to occupy one of the two inter-crossing SC structures [13, 17, 22, 25] as depicted in figure 1. As pointed out by Landau [17], this symmetry breaking from FCC to SC is a strong indicator of a second order phase transition, and a suitable order parameter can be defined as the difference of species concentration between each of the inter-crossing SC lattices. This has been demonstrated experimentally by using not only neutron diffraction but also high resolution x-ray scattering [18]. Although the prototype system is stoichiometric 1 : 1  $\beta$ -brass, this type of

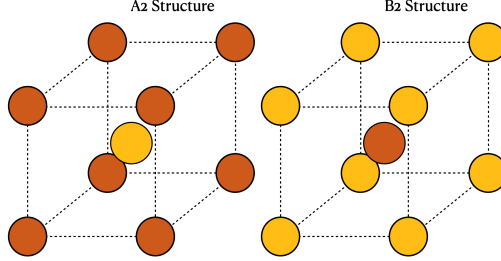


Figure 1: Intercrossing SC structures after BCC symmetry breaking in binary alloys. While  $m_\alpha$  defines the concentration of orange atoms in the A2 structure,  $m_\beta$  defines the concentration of yellow atoms in the B2 structure [22].

brass can be found for concentrations of Zn down to 35% per weight [10]. Moreover, varying species concentration on an alloy can dramatically alter its mechanical, thermal and electrical properties [10]. Hence, following Porta and Tastan [22], studying the influence of species concentration in binary alloys with BCC structure similar to  $\beta$ -brass is justified.

Therefore, in what follows, it is to be assumed that the system discussed is a binary alloy  $A_xB_{1-x}$ , with BCC lattice symmetry and non-stoichiometric proportions. As mentioned in [6], ordering is due to redistribution of atoms in the lattice that yields a minimum of free energy of the alloy. According to [22, 6], the most important ordering mechanism is diffusion of atoms through the lattice due to thermal excitation. Prototypical  $\beta$ -brass is a substitutional alloy [6]. This implies that atom diffusion is mainly caused by the existence of vacant lattice sites. In this type of solid solutions, an atom vibrating in a fixed lattice site can jump to a vacant neighbouring site if it has enough thermal energy, thus reshaping the local species concentration [6]. This fact, though of great importance, is not explicitly considered in simple statistical models of binary alloys [16, 1, 3, 13, 13]. However, this is extensively developed in more accurate models considering kinetics of domain growth in quenched alloys [19]. As a matter of fact, in [22] Porta and Tastan highlight the importance of vacant lattice sites, even though the model presented for a binary alloy does not take that explicitly into account.

Following [22, 13, 25], due to the large timescale of diffusion processes in solid solutions as opposed to lattice vibrations, for example, the interaction energy can be reduced to the summation of bond energy between nearest neighbour (nn) atom pairs. This leads to the definition of an interaction Hamiltonian:

$$H = \frac{1}{2}(\epsilon_{AA}V_{AA} + \epsilon_{AB}V_{BB} + \epsilon_{BB}V_{BB}) \quad (1)$$

Where  $\epsilon_{\alpha\beta}$  is the bond energy between atoms of species  $\alpha$  and  $\beta$ , and  $V_{\alpha\beta}$  is the number of (ordered) nearest neighbour (nn) pairs of bonds involving atoms of species  $\alpha$  and  $\beta$ . This Hamiltonian can be rewritten in terms of a lattice variable [22, 13, 25]

$$C_i = \begin{cases} 1, & \text{if lattice point } i \text{ is occupied by an atom of species A} \\ 0, & \text{if lattice point } i \text{ is occupied by an atom of species B} \end{cases}$$

As follows:

$$H = \sum_{\langle ij \rangle} \left[ C_i C_j \epsilon_{AA} + (1 - C_i)(1 - C_j) \epsilon_{BB} + (1 - C_i)C_j \epsilon_{AB} + C_i(1 - C_j) \epsilon_{BA} \right] \quad (2)$$

Where  $\langle ij \rangle$  denotes summation over nearest neighbour lattice points. Consider the change of lattice variable  $S_i = 2C_i - 1$ . In terms of this new lattice variable with explicit definition

$$s_i = \begin{cases} 1, & \text{if lattice point } i \text{ is occupied by an atom of species A} \\ -1, & \text{if lattice point } i \text{ is occupied by an atom of species B} \end{cases}$$

It is possible to show that the lattice Hamiltonian can be written as [13, 22]

$$H = E_0 - J_{AB} \sum_{\langle ij \rangle} s_i s_j - h_{AB} \sum_i s_i \quad (3)$$

With the identifications:

$$E_0 = \frac{Nz}{4} (\epsilon_{AA} + 2\epsilon_{AB} + \epsilon_{BB}) \quad (4)$$

$$J_{AB} = \frac{1}{4} (2\epsilon_{AB} - \epsilon_{AA} - \epsilon_{BB}) \quad (5)$$

$$h_{AB} = \frac{z}{2} (\epsilon_{BB} - \epsilon_{AA}) \quad (6)$$

Where  $N$  is the number of lattice sites, and  $z$  is the coordination number of the lattice. Two important remarks need to be made regarding the summations involved in Hamiltonian 3. The first one is that for fixed concentration of species A,  $x$ , lattice variables are constrained to

$$\frac{1}{N} \sum_i s_i = \sum_i (2C_i - 1) = 2x - 1 \quad (7)$$

It will be shown in the next subsection that this restriction can be taken into account by studying the system in the context of the grand canonical potential. On the other hand, by examining the parameter  $J_{AB}$  it can be intuited that if  $J_{AB} < 0$ , the ordering in the alloy favours formation of A-B bonds [22, 6]. If, on the contrary,  $J_{AB} > 0$ , the ordering favours formation of A-A or B-B bonds [22, 6]. It can be demonstrated via thermodynamic arguments [6] that if  $J_{AB} = 0$ , no heat of solution is required, and no ordering at low temperatures takes place.

In summary, order-disorder transitions in binary alloys  $A_x B_{1-x}$ , following the prototype of  $\beta$ -brass, can be modelled using lattice variables that yield a Hamiltonian akin to 3. This Hamiltonian is valid as long as vacancy-assisted diffusion is not explicitly considered, and thermal variation of parameters 6 due to, for example, thermal lattice vibrations are ignored [13, 22, 25]. Moreover, parameter  $J_{AB}$  determines the type of ordering, and considering the prototypical  $\beta$ -brass, it is desired that  $J_{AB} < 0$ .

## 2.2 Second Order Transitions: Fundamental Ideas

Second order transitions usually happen when a continuous change of state of a system takes place, and cooling below a certain critical temperature (for a particular value of another intensive variable) breaks an existing symmetry of the system [17, 12]. In the case of binary alloys with BCC structure, at high temperatures, each species of atoms occupy with equal probability all lattice sites. However, below the critical temperature atoms of same species tend to occupy one of the two intercrossing SC lattices inside the BCC structure [17, 22]. From a statistico-thermodynamic point of view, phase transitions of this kind occur with continuous change in extensive quantities [12], their first derivatives (for example specific heat) present a discontinuity at the transition or critical point though [17]. A hugely important quantity known as the order parameter acquires a non zero value for temperatures below the critical one, and is zero for higher values of temperature. The order parameter reflects the symmetry breaking below the critical point. In the case of binary alloys, the symmetry of the BCC lattice is broken, leading to a SC symmetry [17]. For this particular system, the following order parameter is defined, see fig. 1 [22]:

$$\eta = \frac{m_\alpha - m_\beta}{2} \quad (8)$$

One of the simplest models that exhibit this features is the Ising model. It was conceived to emulate magnetic solids that present a ferromagnetic (antiferromagnetic) transition when cooled below a critical temperature, and in the presence of an external magnetic field below a critical value. Correlation in the system is due to spin ( $\mathbf{s}_i$ ) interaction between nearest neighbours in a lattice. It is assumed that degrees of freedom are spin-half ( $\mathbf{s}_i = \pm \mathbf{e}_z$ ). The microscopic hamiltonian that characterises the interaction is [12]:

$$H = -J \sum_{\langle ij \rangle} \mathbf{s}_i \cdot \mathbf{s}_j - \mathbf{h} \cdot \sum_i \mathbf{s}_i \quad (9)$$

Where  $\mathbf{h}$  is an external magnetic field and the first sum is carried over nearest neighbours in the solid lattice. The parameter  $J$  determines whether the solid experiences a ferromagnetic phase ( $J > 0$ ) or an antiferromagnetic phase ( $J < 0$ ) [12, 22, 5]. For this particular system, the magnetisation per unit particle, statistically defined as

$$\mathbf{m} = \frac{1}{N} \sum_i \mathbf{s}_i \quad (10)$$

can be taken as the order parameter of the system. Below the critical point ( $h_c, T_c$ ), the system has a long-range correlation between interacting spins (all aligned or anti-aligned), thus leading to an ordered state. In the absence of external magnetic field, phase transition when cooling leads from zero net magnetisation above critical temperature, to a finite magnetisation below that temperature. Near the transition point, the order parameter can acquire arbitrarily small values, and the free energy proves to be an important tool to understand quantitatively the phase transition [17, 22, 12, 4, 24]. A series expansion of the free energy in the order parameter (imposing a restriction on the minima of the free energy) leads to analytical calculations of critical temperatures and, in the case of the Ising Model, a relation between magnetisation and external magnetic field near the critical point [12]. In 1944, Onsager derived the mentioned relations for a two-dimensional Ising Model [5]. However, the particular formalism of mean field approximations used to study higher-dimensional models will be discussed in the context of order-disorder transitions in binary alloys,

as in [22]. For now, the notion of critical exponents and correlation function will be introduced in the context of the Ising model, since they present a quite intuitive picture of second order phase transitions [12].

From the Ginzburg-Landau theory of phase transitions, it can be shown that thermodynamic quantities such as specific heat or thermal compressibility experience a divergence near the transition [17, 12]. This divergence usually follows a power law. In the particular case of magnetic system modelled via Ising hamiltonian (eqn. 9), the specific heat and magnetic susceptibility follow the laws [12]

$$c_H \sim |1 - T/T_c|^{-\alpha} \quad (11)$$

$$\chi_H \sim |1 - T/T_c|^{-\gamma} \quad (12)$$

An important indicator of the order-disorder transition of a system is the correlation function, which gives information about how the local order parameter in a certain point on the lattice is correlated with its value at a distance  $r$  apart. According to [12], the correlation function can be described, above critical temperature, by the expression

$$G(r, T) \sim \exp\left[-\frac{r}{\zeta(T)}\right] \quad (13)$$

where  $\zeta(T)$  is called correlation length. This quantity determines the extension of the local order in the system. Near the transition point, correlation function and length diverge following power laws of the form [12]

$$G(r, T) \sim \frac{1}{r^{d-2+\sigma}} \quad (14)$$

$$(15)$$

$$Pi(T) \sim |1 - T/T_c|^{-\nu} \quad (16)$$

where  $d$  is the dimension of the lattice. Below the critical point, the correlation function takes a constant value, and local differences with the asymptotic value are characterised by the correlation length [12]. In summary, critical exponents, namely  $\nu, \sigma, \alpha, \gamma$ , describe not only the divergence of thermodynamic quantities, but also the order extension below critical temperature. Numerical simulations of the two-dimensional Ising model carried out in [12] show how the first derivatives of thermodynamical potentials (such as magnetic susceptibility and specific heat) present a divergence near the critical point of phase transition, and the order parameter acquires non zero value in the ordered phase (below critical temperature). Moreover, this work also illustrates that correlation between points of the system is increased as the system is cooled to the critical temperature, thus depicting a characteristic feature of second order phase transitions: divergent correlation length near the critical point (fig. 2). In table 1, some of the computed critical exponents for 2D and 3D Ising Models. The exponent  $\alpha = 0$  means a logarithmic divergence rather than a power law.

As established in [22] and [13], the Ising model dynamics can be translated to other systems than magnetic solids. Specifically, it can be used to treat phase transitions in binary alloys of the form  $A_x B_{1-x}$ . In subsection 2.1 it was shown that interaction between atoms, under certain restrictions, leads to an Ising hamiltonian like eqn. 9. In this model,  $J < 0$  favours the formation of

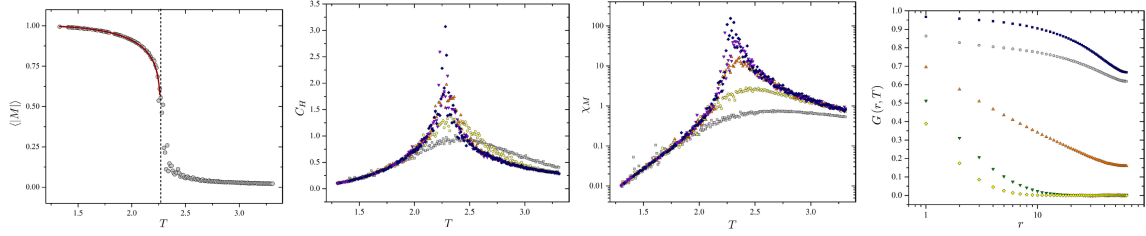


Figure 2: From left to right. (1) Magnetisation as a function of temperature, notice sudden increase below critical temperature. (2) and (3) specific heat and susceptibility as function of temperature, notice divergence near critical temperature. (4) Correlation function for temperatures below critical point (blue squares and gray dots) and above critical point (the rest), notice that at low temperatures the correlation length is quite large [12].

Exponent	2D Model	3D Model
$\alpha$	0	0.11008(1)
$\gamma$	$3/4$	1.2370775(10)
$\nu$	1	0.629971(4)

Table 1: 2D Ising Exponents were computed analytically following Onsager's solution, and Monte Carlo Simulations carried out by Ibarra-García-Padilla et. al [12] show excellent agreement for a square lattice. Exact analytical solution of the 3D Ising Model is not yet known, and exponents for a SC lattice are presented [23, 14].

AB pairs, while  $J > 0$  favours formation of AA and BB pairs. Since the model is devised to study order-disorder transitions as described at the beginning of the section, it is assumed that  $J < 0$  [22]. Since the system is restricted by the constraints

$$\sum_i C_i = N_A = Nx \quad (17)$$

$$\sum_i S_i^2 = N \quad (18)$$

where  $N_A$  is the total number of atoms of the species A, the partition function in the canonical ensemble is restricted to a sum over the states that conform to those conditions

$$Z = \sum_{\{S_i\}^*} \exp(-\beta H) \quad (19)$$

In order to perform a simpler statistico-thermodynamic analysis of the system, the grand canonical partition function may be computed. By definition of the grand partition function

$$Q = \sum_{N_A=0}^N \exp\{-\beta(H - \zeta N_A)\} \quad (20)$$

where  $\zeta$  is the chemical potential difference  $\mu_A - \mu_B$ , it is evident that in this ensemble all lattice configurations must be included, provided the Hamiltonian is transformed as follows

$$H \rightarrow H - \zeta N_A \quad (21)$$

In [22] is shown that this is equivalent to changing the alloy Hamiltonian by the identifications

$$h \rightarrow h + \frac{\zeta}{2} \quad (22)$$

$$E_0 \rightarrow E_0 - \frac{N\zeta}{2} \quad (23)$$

Therefore, the partition function used to study the Ising model in the canonical ensemble, can be used to study a binary alloy in the grand canonical ensemble by relating the chemical potential to the external magnetic field and an offset energy [22]. Although, from a physical point of view, this corresponds to putting the system in contact with an ideal particle reservoir, which is not consistent with how actual experiments are performed, in [22] is alleged that this facilitates analysis using results from the well-known Ising model, and simplifies numerical simulations.

### 2.2.1 Mean Field Approximations in the Ising Model

Since analytic solution for the Ising model in more than two dimensions is not known, qualitative statistico-thermodynamic analysis can be performed by neglecting deviations from the mean value of  $S_j$  in the neighbourhood of a given lattice point  $i$  [22]. This decouples the alloy hamiltonian and simplifies greatly the calculation of thermodynamic potentials. Although a standard decoupling of the Ising Hamiltonian is presented in [12], this calculations are not immediately translated to the binary alloy system since the order parameter is not as straightforward (see eqn. 8). Two auxiliary variables are to be defined [22]:

$$m_\alpha = \frac{2}{N} \left\langle \sum_{i \in A_2} S_i \right\rangle = \langle S_i^\alpha \rangle \quad (24)$$

$$m_\beta = \frac{2}{N} \left\langle \sum_{i \in B_2} S_i \right\rangle = \langle S_i^\beta \rangle \quad (25)$$

Considering a point in the lattice substructure  $A_2$  (fig. 1), and assuming that neighbouring points have  $S_j = \langle S_i^\beta \rangle$ , the hamiltonian for points in this substructure can be decoupled to [22]

$$H_i = -S_i(zJm_\beta + h) \quad (26)$$

Analogous expression can be obtained for lattice points in the  $B_2$  substructure. This allows straightforward computation of the one-particle partition function, and thus macroscopic observables [22]. Two results are of remarkable importance. The first one is an elementary expression that relates  $m_\alpha$  to the chemical potential at a given temperature

$$m_\alpha = \tanh(\beta[zJ \tanh(\beta(zJm_\alpha + h(\zeta))) + h(\zeta)]) \quad (27)$$

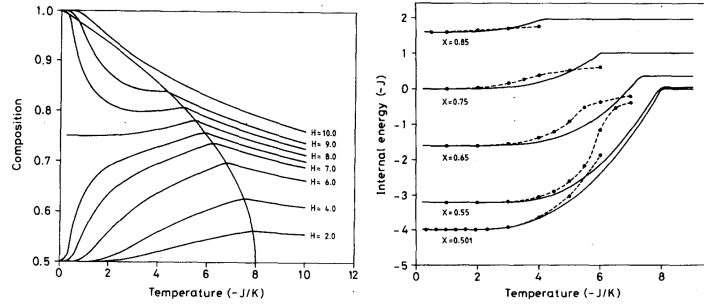


Figure 3: From left to right. (1) Phase space section in the plane  $x - T$ , the solid vertical curve corresponds to the set of critical points. (2) Internal energy as a function of temperature for several compositions, the discontinuities in the derivative on each curve indicate critical temperatures [22].

an analogous expression can be found for  $m_\beta$ . The second is an expression that relates the chemical potential to the temperature at a critical transition point

$$h(\zeta) = k_B T \tanh^{-1} \left[ \sqrt{1 + \frac{k_B T}{z J}} \right] - z J \sqrt{1 + \frac{k_B T}{z J}} \quad (28)$$

Using equations 28 and 27, it is possible to estimate the location of the critical curve in the projection of the phase space  $x - T$  [22]. This curve is of immense theoretical value, since, when compared to experimental data, it can give information about the strengths and weaknesses of the model. An example of the results obtained in [22] is shown in figure 3. Numerical simulations were performed and compared to the mean field approximation.

### 2.3 Spin-1 Models for Binary Alloys

Although the model describes interesting dynamics, and exhibits a second order phase transition, it is suggested that the model be enriched with more complexities in the interaction hamiltonian [22]. In particular, from the discussion on section 2.1, it is suggested that it include vacancy-assisted ordering. Since ordering in an alloy is a diffusion process, impurities and vacancies in lattice sites play an important role in the dynamics of the phase transition. Generalising the Ising Model from spin-half to spin-one, might make possible to include vacancies or holes as an extra spin state in a lattice site. This can be done by defining a lattice variable

$$S_i = \begin{cases} 1 & \text{if site is occupied by atom of species } A \\ 0 & \text{if site is occupied by vacancy} \\ -1 & \text{if site is occupied by atom of species } B \end{cases} \quad (29)$$

The most straightforward generalisation is suggested in [12], and corresponds to conserving the Hamiltonian 9, but allowing the spin to take values  $-1, 0, 1$ . On the other hand, a more appropriate model, namely Blume-Emery-Griffiths (BEG) model [4], extends the Hamiltonian to include not only the bilinear spin-one interaction, but also quadratic and biquadratic interactions. It has

been used successfully in modelling multicritical phenomena in mixtures of  $\text{He}^3 - \text{He}^4$ . The BEG Hamiltonian is:

$$H = -J \sum_{\langle ij \rangle} S_i S_j - K \sum_{\langle ij \rangle} S_i^2 S_j^2 - \Delta \sum_i S_i^2 \quad (30)$$

As pointed out in [4], this model is suitable for mean field approximations. In addition to that, numerical simulations performed in [24] and [4] show the existence of a critical triple point, and first order phase transitions for some parameter values. In the context of magnetic solids, [24] proposed a second order parameter to describe phase transitions to the denominated staggered quadrupolar phase:

$$Q = \frac{2}{N} \left\{ \sum_{i \in A_2} S_i^2 - \sum_{i \in B_2} S_i^2 \right\} \quad (31)$$

In this phase, one of the sub-lattices is occupied by vacancies, and the other is occupied by atoms of type A or B. In figure 4, results of numerical simulations from [4] and [24] are presented. Although analytical calculations in the mean field approximation were performed in [4], explicit calculations of quantities such as specific heat are not carried out. On the other hand, [24] presents only numerical simulations. More generally, according to [1] order parameters

$$m_\omega = \frac{1}{N} \left| \sum_{i \in \omega} S_i \right| \quad (32)$$

$$q_\omega = \frac{1}{N} \sum_{i \in \omega} S_i^2 \quad (33)$$

where  $\omega$  stands for one of the inter-crossing sublattices in the alloy crystal structure, can characterise the possible orderings in a binary alloy. From a physical perspective, for binary alloys that present an ordering transition akin to  $\beta$ -brass, each of the constants  $J, K, \Delta$  determine atom-atom interaction, atom-vacancy interaction and asymmetry in the system introduced by the interaction between vacancies and boundaries of domains with a finite size [19]. Following work performed in [19], the last term on the interaction Hamiltonian can be neglected for binry alloys such as those intended to be described in the present project. This is equivalent to neglecting the energy difference between A-A and B-B pairs [19]. Therefore, the BEG Hamiltonian that is to be used to model the influence of vacancies in the order-disorder transitions of binary alloys with BCC lattice structures is:

$$H = -J \sum_{\langle ij \rangle} S_i S_j - K \sum_{\langle ij \rangle} S_i^2 S_j^2 \quad (34)$$

It shall be assumed that  $J < 0$ , so that bonds A-B are favoured. Given that the 3D Ising Model has proved to be a remarkably good model for ordering in binary alloys [16, 14, 23], and following the insights of [19], it shall be assumed that  $K/J > 1$ . This corresponds to repulsion between vacancies.

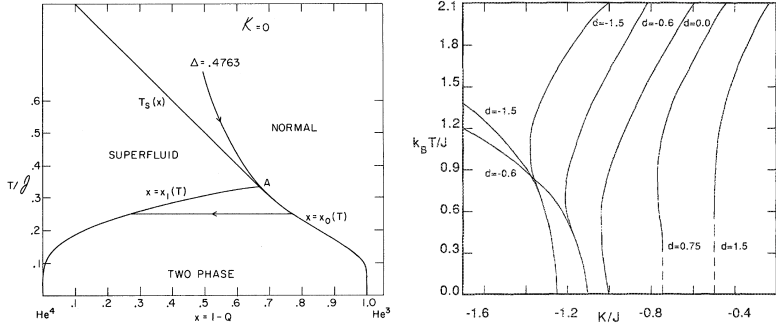


Figure 4: From left to right. (1) Multicritical phenomena illustrated in the phase space projection on the  $x - T$  plane for a mixtures of  $\text{He}^3 - \text{He}^4$  [4]. (2) Critical curves for magnetic solids in the BEG model in the phase space projection on plane  $K - T$  [24].

## 2.4 Monte Carlo Simulations: Fundamental Ideas

In a nutshell, Monte Carlo simulations in statistical thermodynamics are tools designed for sampling a system's state space according to a desired probability distribution (i.e. Gibbs distribution), in order to compute expectation values that correspond to macroscopic observables [12]. The state space of a particular system is quite big though. This implies that a clever algorithm for sampling the probability density of states in phase space is needed. In general, a Markov chain is generated so that the equilibrium distribution approaches the desired probability density [12, 15].

The Metropolis-Hastings algorithm is a solution to the problem of generating a Markov chain that converges to a particular equilibrium distribution. It is based on the detailed balance condition [15, 12]. The algorithm is as follows [22]:

1. Propose a change of system configuration from  $n \rightarrow m$ .
2. Compute the energy difference  $\Delta H = H\{m\} - H\{n\}$ .
3. Compute the acceptance probability  $W = \min(1, \exp[-\beta\Delta H])$ .
4. Select a random number  $\kappa$  between 0 and 1. If  $\kappa \leq W$ ,  $m$  is accepted as a new configuration of the statistical ensemble. Otherwise, the configuration of the system remains as  $n$

These steps are repeated as many times as lattice points are considered. After that, observables of interest (such as internal energy or order parameter) are computed for the current configuration. This completes a Monte Carlo Step. Eventually, the time series of observables are averaged to compute the statistical observables [12, 22]. As discussed before, long correlation lengths occur near the critical point in the Ising Model. This leads to large correlation times in Monte Carlo simulation of the phenomenon, something called critical slowdown [12, 15]. In this regime, changing the configuration of the system (i.e. flipping a spin) is more difficult, and hence the computation of statistical averages over an ensemble. In principle, Metropolis-Hastings algorithm converges to correct statistical averages (within statistical errors off course). However, the number of steps required depends on the temperature of the system [12]. More sophisticated algorithms with faster convergence such as Heat Bath sampling [15], which flips a spin randomly according to a local

external field, or Importance sampling [15, 22]. In references cited throughout this section, specially on [15], particular details on the implementation of Markov Monte Carlo simulations of the Ising Model can be found.

For computing statistical averages, which lead to description of thermodynamic observables such as internal energy, specific heat or order parameter, some care must be taken. In [12] and [15], computation of observables using statistico-thermodynamic identities such as

$$c_H = \frac{1}{k_B T^2} (\langle E^2 \rangle - \langle E \rangle^2) \quad (35)$$

are strongly recommended. Since Markov chains have finite correlation time in general, some Monte Carlo steps must be wasted before converging to the desired equilibrium distribution. In [22], from 5000 Monte Carlo Steps, the first 500 were not used in order to obtain more accurate statistical averages.

Concerning the implementation of the algorithm, in order to avoid border effects, periodic boundary conditions on the lattice must be imposed [12]. Also, when considering nearest neighbour interaction, spin-flipping probabilities can be computed a priori to speed up the simulation. Needless to say, a good random generator must be available in order to have decent accuracy. When considering finite size lattices, the correlation length and other important quantities tend to scale according to the size of the lattice. This is called finite-size scaling [12]. There are techniques to rescale important quantities due to finite-size effects, they are not very precise due to critical slowdown though [12].

Since the project is oriented towards studying a system with constraints in its space state (eqns. 18), a particular algorithm for spin flipping that respects those limitations must be implemented. By working in the grand canonical ensemble, those limitations can be avoided [22]. Nevertheless, an alternative option is using Kawasaki dynamics, which flips a pair of spins at a single Monte Carlo steps in such a way that the constraints are preserved. Successful application of this dynamics to the numerical study of some properties of phase separation in binary alloys is presented in [3]. However, the model developed built upon the standard Ising Model with a constraint on the number of particles, somewhat in the spirit of [22].

Determination of critical temperature might follow finite size scaling technique depicted by Ibarra and others [12]. As is described in their work, curves of magnetization shall be computed for fixed  $\mu$  and  $\zeta$ . Since the simulated system is of finite size  $L \times L$ , there is no discontinuity of first derivatives in an ordering transition. This happens because correlation length cannot diverge, but is limited to the size of the simulated lattice [12, 25]. As the lattice size increases, the first derivatives of thermodynamic quantities tend to diverge at a temperature  $T_c(L)$ , that depends on the lattice size. According to Ibarra and others, the relation between critical temperature and lattice size is given by

$$T_c(L)^{-1} - T_c(\infty)^{-1} \propto L^{-\frac{1}{\nu}}$$

Notice that critical temperature can be inferred by performing a power law regression of a set of points  $T_c(L)^{-1}$  vs.  $L^{-1}$ . This is carried out successfully by Ibarra and others [12]. A demonstration of the results is shown in figure 5.

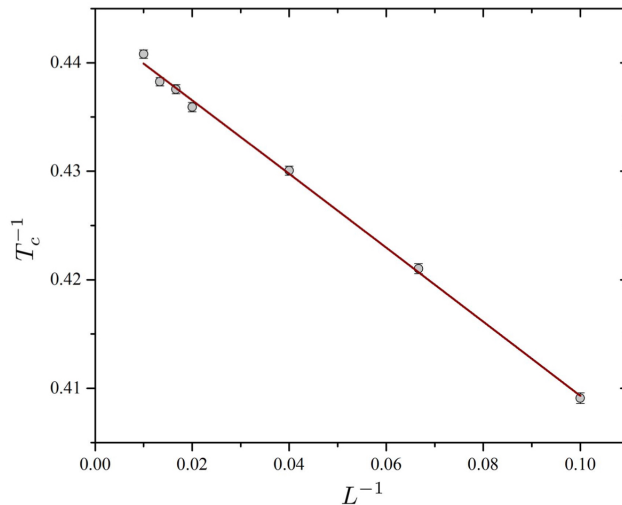


Figure 5: Power law fit performed by Ibarra to compute critical temperature of 2D Ising Model.

### 3 State of the Art

The history of the study of the Ising model goes back to 1925's Ising's doctors dissertation [20]. This model was proposed to investigate ferromagnetism. Ising himself derived a solution for Hamiltonian 9 in a one-dimensional system [12]. On 1944, Onsager derived a solution for a two-dimensional square lattice that exhibits all fundamental aspects of second order phase transition discussed in section 2 [2, 2]. Although it is currently assumed that this interaction is an oversimplified approach to ferromagnetism, it was shortly realised that its rich behaviour could be extrapolated to other physical systems. On Newell and Montroll's review of the Ising Model of ferromagnetism, dating back to 1953, an explicit equivalence between Ising model and order-disorder transitions in substitutional binary alloys is presented on appendix 1 [20]. Hence, not very long after Onsager's emblematic solution, the history of the study of ordering transitions in binary alloys and the ferromagnetic Ising model got together.

As pointed out on [14], in spite of the several difficulties in studying experimentally the order-disorder phase transitions in substitutional binary alloys, it has been shown via high resolution x-ray diffraction that this phenomenon can be accounted for by a three-dimensional Ising Model. In past experimental works, critical exponents associated to heat capacity have been measured for  $\beta$ -brass near stoichiometric proportions 1 : 1 [16]. Given that no exact solution for the three-dimensional Ising model is known, these measurements are sometimes used as reference for numerical calculations using mechanic-statistical techniques [8]. Although successful in describing general properties of ordering in binary alloys, nuances concerning the influence of vacancy-assisted diffusion on the kinetics of this process have been pointed out over the last half century [19, 7].

Investigations on order-disorder transformations in the body-centred cubic structure using the Monte Carlo Method, performed by P. A. Flinn and G. M. McManus indicated that jumping of vacancies to second neighbour positions are influential in the kinetics of the transformation [21]. Effects of vacancies in a lattice have been studied by Vives and Planes [7]. Their model consisted on

a 3D Ising Hamiltonian in which a single atom was substituted by a vacancy. Using Monte Carlo simulations, they showed that the power laws characterising the increase of correlation length with time during phase transition is drastically affected by the presence of vacancies [7]. Therefore, the inclusion of vacancy-assisted diffusion is relevant for the study of binary alloys, even though the conventional spin-1/2 3D Ising Model seems to give pretty good account of the main features of ordering in binary alloys.

As pointed out in section 2, a spin-1 Ising model might be used to take into account vacancy diffusion. The canonical Blume-Emery-Griffiths model has arisen as a suitable generalization. Presented in 1971 to study  $\lambda$  transitions in  $\text{He}^3 - \text{He}^4$  mixtures [4], its applications range from pure mathematical study to direct application in kinetics of ordering in binary alloys. In [11], famous exact computation of partition function for the honeycomb lattice, performed by Horiguchi, is presented. On the other hand, study of the effects of vacancy interaction on domain growth in a two-dimensional lattice, using the BEG Hamiltonian 34, carried out by Porta, Frontera, Vives and Castan [19], has thrown light into the parameter  $K, J$  phase space and how it determines the interactions between anti-phase boundaries and mobile vacancies. More recently, Ozkan and Kutlu have applied the FCC lattice BEG model to study ordering in stoichiometric Cu-Au type structures in the staggered quadrupolar region [1].

## 4 Statement of the Problem

As mentioned on section 2, the present project is building upon insights from [12] and [22]. The physical foundations for the analysis of a binary alloy are presented on the former reference, whereas the general aspects of second order phase transitions and, specifically, of the mean field approximation for the general magnetic Ising model are presented in the first reference. Porta and Castan build upon the mean field approximation for the Ising model to gain insight into the projection of critical surfaces onto the  $x - T$  plane corresponding to a binary alloy, as discussed before[22]. On the other hand, Ibarra et. al. [12], use a mean field approximation to gain insight into the critical exponents for a 2D Ising Model. The mentioned references are complementary to one another in the sense that Porta and Castan [22] provide an application of the Ising model to a physical system such as a binary allow with BCC symmetry, whereas Ibarra et. al. provide the general framework for studying second order phase transitions using an Ising model, emphasising on the importance of critical exponents and correlation length to characterise them, and the details of implementing numerical simulations using Monte Carlo Methods.

Regarding possible further developments, on the first reference, it is suggested on section 9.2 that BEG model be studied as an interesting generalisation of spin-half Ising model. In particular, calculation of thermodynamic quantities such as internal energy, magnetisation, specific heat and magnetic susceptibility is advised [12]. On the second reference, section II, the importance of vacancies in the ordering of a binary alloy is pointed out, not developed further though. Since the inclusion of holes as a possible state of a lattice point in an alloy can be carried out by considering spin-one interactions, the BEG model stands out as a suitable candidate for further analysis. Not only has it been used successfully in describing phase transition on liquid mixtures [4], but also has shown interesting behaviour for magnetic solids as well [24].

Therefore, the problem set up in this project is the characterisation of vacancy-assisted second order phase transitions in 2D binary alloys with bipartite lattice structure at high temperatures, using the BEG model discussed in section 2, by determining the effects on the critical curves in the  $x - T$  and  $\zeta - T$  planes, produced by a small concentration of vacancies  $c_v \approx 1 \times 10^{-4}$ . As

mentioned in subsection 2.1, simple spin-1/2 Ising models, though successful in describing some features of order-disorder transitions in binary alloys following  $\beta$ -brass prototype, do not take into account explicitly the fundamental diffusion mechanism involved in substitutional alloys. As a result, the inclusion of this factor into the phase transition might be a step towards a more accurate understanding of ordering in this type of solid metallic solutions.

Following the spirit of [22] and [4], the study of phase transitions will be performed mainly on the  $x - T$  and  $\zeta - T$  projections of the phase space. Hence, by careful study of thermodynamic quantities that show special behaviour at transition points (i. e. specific heat, order parameters, internal energy) for given vacancy chemical potential  $\mu$ , numerical and analytical estimation of critical curves in the mentioned phase space projection will be obtained. Vacancy concentration will be included by the definition of an external field, following Porta and Castán [22]. After explicitly demonstrating that the interaction Hamiltonian 1 can be mapped to a BEG Hamiltonian, analysis in a mean field approximation is to be performed in order to study qualitatively the boundary for ordering transitions. This process shall follow the scheme depicted in [12]. Given that in the BEG model for a bipartite lattice two order parameters are relevant [1], this rough estimate will be computed only for magnetisation (see eq. 8). This restriction is imposed by the experimentally observed nature of order-disorder transitions in alloys such as the ones discussed in section 2. In a manner similar to [22], the statistico-thermodynamic study of the system will be performed in the grand canonical ensemble, and results from magnetic BEG model derived following [12] are to be extrapolated correspondingly. From this extrapolation, mean field expressions relating chemical potential, equilibrium species concentration and critical temperature are to be used in order to determine  $x - T$  critical curves. This shall be based upon the insights of [22]. The curves obtained will be compared to those obtained by [22]. Since mean field approximations are of limited validity [25], Monte Carlo simulations will be performed in order to establish better estimates of the critical curves in the  $\zeta - T$  plane. Critical points are to be determined following the finite size scaling technique presented on [12].

## 4.1 Analytical Component of the Problem

The analytical component of the problem is directly related to the study of the BEG Hamiltonian 34 in a mean field approximation. The first step is to demonstrate mathematically that interaction Hamiltonian 3 can be mapped to a BEG Hamiltonian following a deduction akin to Porta and Castan's [22]. Due to restrictions imposed by the equilibrium concentration of the prototypical system to be studied, statistical analysis is to be performed in the grand canonical ensemble. An effective Hamiltonian that involves chemical potential is to be derived, and mapped onto the general BEG model Hamiltonian. Following this mapping process, a general mean field approximation of the BEG model shall be performed, following a process similar to [12]. Using a local decoupled Hamiltonian, the free energy will be derived following steps reminiscent of Ibarra et. al. [12]. By minimising free energy with respect to order parameter, expressions for the critical temperature, magnetisation near critical point, and heat capacity near critical point will be derived. From this expressions, mean field critical exponents are to be read off and compared to the values in table 1.

Once the mapping of the binary alloy Hamiltonian to the BEG model has been mathematically demonstrated, extrapolation to the particular system of a 2D binary alloy bipartite lattice structure exhibiting phase transitions akin to  $\beta$ -brass will be performed following Porta and Castan's approach [22]. By using a decoupled Hamiltonian based on the general approach taken following [12], equations analogous to 27 and 28 shall be derived. From this equations, a general expression

that relates chemical potential, equilibrium concentration and critical temperature should be derived. Finally, from these equations, mean field critical curves in the  $x - T$  plane should be found, thus relating critical temperature to composition. Given the expected nature of the equations, it is very probable that this last step implies a numerical solution consisting on implementing an elementary root finding algorithm.

## 4.2 Numerical Component of the Problem

In order to study order-disorder transitions, Monte Carlo Simulations will be performed. Since a 2D bipartite<sup>1</sup> lattice will be considered, lattices with up to approximately  $64 \times 64$  unit cells will be considered. In [22] more unit cells were simulated, however, due to the increase on states of the system, this number seems appropriate a priori [24]. Following the spirit of [12], numerical calculations of internal energy, order parameters and specific heat will be performed for fixed large negative value of vacancy chemical potential, and several values of atom chemical potential difference. Emphasis will be given to illustrating the discontinuity of some of those quantities at the critical point. With this computations, critical curves in  $\zeta - T$  plane will be determined, and compared to those obtained in the mean field approximation. Determination of critical temperature for given values of  $\zeta$  and  $\mu$  will follow finite size scaling technique depicted by Ibarra and others [12].

From a computational point of view, a proper algorithm will be chosen for sampling Gibbs distribution for the BEG Hamiltonian. In principle, and following [12], Metropolis-Hastings algorithm could be used. However, some faster methods like importance sampling or heat-bath sampling could be used [15]. Therefore, a first step towards simulating phase transitions is choosing a proper sampling algorithm. Computation of expected values of observables will be performed using statistical averages and not thermodynamic derivatives. Restrictions on atom concentration will be taken into account by the chemical potential differences  $\mu$  and  $\zeta$ .

## 5 Motivation and Relevance

The study of the dependence of thermal, mechanical and electrical properties of solid solutions with composition is paramount for the development of new materials. This is not only valid for semiconductor devices, as commented on [10] by altering the concentration of Zn in brass, an  $\alpha$  phase can be obtained that can be worked cold, has an FCC structure, and is weaker yet more malleable than  $\beta$ -brass. Equally important, the study of vacancy diffusion mechanisms in ordering transitions of binary alloys is relevant for manufacturing processes that rely on quenching. As demonstrated in [19], vacancy interactions are determinant in domain growth, and thus in the mechanical properties of an alloy after treated by quenching.

From an academical perspective, Ising type models present a very rich and broad approach to second order phase transitions. No exact analytical solution for general Ising-like Models is known, and hence the present project is an opportunity to discuss the main features of a problem that is still of active research in physics [9, 14, 23]. Furthermore, this project presents the opportunity to review important techniques used in the analysis of lattice models in statistical physics, both computational and purely mathematical.

---

<sup>1</sup>The lattice to be considered will be centered rectangular.

## 6 Objectives of the Project

From section 4, the general objective of the project is to study the effects of vacancy-assisted order-disorder transitions in binary alloys  $A_xB_{1-x}$  forming a bipartite lattice, on  $x - T$  and  $\zeta - T$  phase space projections, by using the BEG model Hamiltonian 34; both from a mean field approximation, and Monte Carlo Simulations. Specific objectives are introduced in this section, that also reflect the expected fate of the project.

### 6.1 Specific Objectives

1. Demonstrate the pertinence and limitations of the BEG Model for describing atomic interaction in a binary alloy by correlating microscopic degrees of freedom and magnetic-related parameters to corresponding quantities in the system of interest.
2. Apply Landau theory in a suitable mean field approximation of the BGE hamiltonian to compute critical curves in  $x - T$  phase space projection, using the appropriate grand partition function, and rough estimates of mentioned critical exponents.
3. Compute specific heat, internal energy and order parameters, as a function of temperature, for different values of  $\zeta$  as statistical averages obtained from Markov Chain Monte Carlo simulations.
4. Identify and locate in  $\zeta - T$  projection of phase space critical points using Monte Carlo simulations and compare to results obtained via mean field approximation.

## 7 Methodology

In this section, specific objectives pointed out in section 6.1 are elaborated. Not only milestones and results will be suggested for each one of them, but also particular references and resources to be used are commented.

### 7.1 Specific Objective 1

The aim of this specific objective is to establish the suitability of Hamiltonian 34. To this end, a simple model that considers atomic interaction characterised by the lattice state variables  $\{S_i\}$  defined in 29 will be derived, assuming that diffusion processes take place in longer timescale than lattice vibrations [22]. Considering that the interaction energy between atoms in neighbouring lattice points should lead to ordering in pretty much the same way as described in [22] or [13], restrictions on the parameters  $J, K$  are to be imposed as discussed on section 2. Those restrictions must take into account the ordering in the denominated staggered quadrupolar phase described in [24]. As pointed out in section 4, although a proper order parameter to describe standard order transition [22, 17], another one must be proposed that accurately describes ordering to the staggered quadrupolar phase. In this phase, one of the sub-lattices is occupied by vacancies, and the other is occupied by atoms of type A or B. In summary, this objective requires two milestones:

1. Derivation of a proper BEG Hamiltonian for a binary alloy with holes and a proper parameter space that allows second order phase transitions.

2. Definition of a second order parameter that describes ordering in the staggered quadrupolar phase described in [24].

This objective is fundamentally related to the analytical part of the problem. Apart from obtaining the mathematical equivalence to a BEG model, this objective starts solid foundations for the mean field approximation. By considering the type of ordering present in the staggered quadrupolar phase, and the parameter range in which transitions to this phase occur, a parameter range can be established so that the only type of order-disorder transitions occur as expected for binary alloys similar to  $\beta$ -brass. The resources employed in achieving this objective are bibliographic references that expose how the standard spin-half Ising Model can be used to describe order-disorder transitions in binary alloys [22, 3, 13]. And also bibliographies references that study the BEG Model [24, 4].

## 7.2 Specific Objective 2

The aim of this specific objective is to take advantage of the formulation of the BEG Model in the grand canonical ensemble to deal with constraints posed by species concentration and apply Landau Theory to compute important thermodynamic quantities near the transition temperature. First of all, a mean field decoupled Hamiltonian should be derived by a process somewhat reminiscent of [22]. The chemical potential should be related to a forcing external field in a way similar to [22]. By computing expected values of  $S_i$ , relations analogous to 27 should be derived. After that, series expansion of free energy near a transition point, should lead to a value of the critical temperature that depends on the parameters of the BEG model and lattice symmetry [12]. Eventually, a relation between the chemical potential, temperature, and order parameter near the critical point should be obtained, pretty much like eqn. 28. From these expressions, numerical calculations via simple root-finding algorithms shall be used to plot mean field critical curves on the  $x - T$  plane. Following the approach of [12] by considering the general BEG Hamiltonian 34, mean field approximation should yield a near-critical-point free energy. In summary, the following milestones are proposed:

1. Find a mean field decoupled Hamiltonian for the BEG Model.
2. Relate chemical potential in the grand canonical description of the model to an external field.
3. Derive analogous relations to eqn. 27 by computing average magnetisation.
4. Perform series expansion of free energy near critical temperature to relate order parameter and critical temperature.
5. Derive analogous relation to eqn. 28 to relate chemical potential and temperature near a critical point.
6. Calculate via root-finding algorithm the critical curves on  $x - T$  plane.
7. Compare calculated curves to results from [22].

As mentioned in the previous subsection, bibliographic references that treat the particular details of Ginzburg-Landau theory are to be used [22, 12, 17, 4]. Since numerical calculations should be performed to compute critical curves, software such as MATLAB or Python 3.x will be used.

### 7.3 Specific Objective 3

The aim of this objective is to implement a Markov Chain Monte Carlo to compute internal energy and order parameters using statistical formulas (such as eqn. 35). A centered rectangular lattice of sizes up to  $64 \times 64$  unit cells should be designed in order to emulate the alloy's dynamic. Glauber dynamics should be implemented following indications from [15]. Also, periodic boundary conditions must be implemented. A suitable sampling algorithm should be chosen. Although [12] suggest using Metropolis-Hastings algorithm for sampling Gibbs distribution, it might be slowly convergent to equilibrium. Therefore, other algorithms such as importance sampling, heat bath sampling and cluster algorithms should be considered also to reduce computation time [15]. Once a Markov Monte Carlo simulation algorithm is settled, specific heat, internal energy and order parameters should be computed via ensemble averages to illustrate the nature of critical points observed. As a remark, mean field approximations should yield parameter values for numerical simulations, specially for temperature and species concentration. In summary, the following milestones are proposed:

1. Encode a centered rectangular alloy lattice.
2. Compute energy difference from spin flipping.
3. Implement Glauber dynamics for spin flipping [15].
4. Select a proper sampling algorithm for Markov Chain Monte Carlo Simulations.
5. Compute internal energy, specific heat and order parameter as function of temperature, for several values of concentration that should be obtained from mean field approximation. Use ensemble expectation values.

For this objective, bibliographic resources are expected to be [15] and [12]. Since this objective is extensive computationally speaking, a good computer and a proper programming language must be used. At the moment, a pc with a 3.4 GHz Quad-Core Intel Core i5 and a Radeon Pro 560 4GB graphics board is available. Programs shall be written in C++, that is not only fast, but also has a proper pseudorandom generator. If more computational resources are needed, CUDA for NVIDIA GPUs can be used via Google Colaboratory.

### 7.4 Specific Objective 4

The aim of this objective is quite clear. In principle, phase transitions of second kind will be identified using the order parameter. They should be checked with specific heat discontinuity and internal energy calculations. For several values of  $\zeta$ , within the range determined using mean field approximation, critical temperature should be determined, and points plotted in  $\zeta - T$  plane. This points shall be interpolated and curves generated compared to analytical approximations and to critical curve from [22]. The milestones for this objective are two:

1. Compute enough critical points (from Monte Carlo simulations) in  $\zeta - T$  plane to perform interpolation of critical curves using Ibarra's approach [12].
2. Compare interpolated critical curves to mean field approximation and results from [22].

The expected resources for this objective are the same as those for the previous one. This objective is paramount to completing the general objective, since, complemented with specific objective 2, leads to an understanding of the chances that the concentration of atoms and of vacant lattice sites induce on the critical temperature.

## 8 Expected Results

Considering the objectives presented in section 6, these are the expected results of the project:

1. Mathematical equivalence between a spin-1 Ising Model, i. e. BEG model, and the bond interaction Hamiltonian 3, in the case of substitutional binary alloy with non negligible vacancy concentration.
2. Mean field expressions akin to 28, 26 and 27 for the Hamiltonian 34, by means of a particularisation of the general framework presented in [12] to the binary alloy system.
3. Curves of heat capacity, order parameter, order parameter derivative and internal energy as a function of temperature, for at least 4 different non-zero  $\zeta$  values.
4. Critical curves on the  $x - T$  and  $\zeta - T$  planes, obtained from mean field approximation and Monte Carlo simulations, respectively. These should be compared to curves presented in [22], in order to determine the influence of a vacancy concentration near  $c_V = 1 \times 10^{-4}$ .

## 9 Schedule

On table 2 are expected times for completion of each objective and milestone. The projected time length of the project is 83 days of work. Milestones marked with (\*) correspond to heavy Monte Carlo Simulations that are supposed to occur simultaneously. Those are the most demanding tasks of the whole project in terms of computational resources and time. It might be the case that these milestones require 10 days more for completion. Hence, the total time length of the project is expected to be between 83 and 93 days. Documentation, report preparation and presentation might include 10 days more, thus an effective time length of 103 days is projected. This correspond to roughly three and a half months of net work.

Work sessions should be daily, and schedule must be adjusted if a milestone is not reached on time. The priority in terms of results are objectives 4 and 5 (see sec. 6.1). If the dynamics of BEG model proves to be too complicated, the model should be simplified to a spin-one Ising Model, and calculations following [12] and [22] are to be carried out. This should be decided before the first week of net work, that is, on achievement of objective 1. If analytic calculations take longer than expected (objectives 1 - 2), parameter values from the reference should be taken as given, and numerical simulations should start after the first month of net work under all circumstances.

## 10 Available Resources

The following are expected bibliographies resources:

- Gogle Scholar Database
- Azure for Students Account granted by Microsoft
- Arxiv Database
- American Physical Society Resources

Objective	Milestone	Time of Completion (Days)
1	1.1	0.5
	1.2	0.5
2	2.1	1
	2.2	1
	2.3	1
	2.4	1
	2.5	0.5
	2.6	0.5
	2.7	0.5
	2.8	0.5
3	3.1	2
	3.2	2
	3.3	3
	3.4	7
	3.5*	32
4	4.1*	32
	4.2*	32
Total Time		58

Table 2: Expected development times of the project. Milestones marked with (\*) are supposed to take place simultaneously.

- American Chemical Society Resources
- Other web resources provided by SINAB from Universidad Nacional de Colombia.

The following are expected computational resources:

- Mac pc with Quad-Core intel Core i5 (3.4 GHz) processor and graphics board Radeon Pro 560 (4 GB).
- Ubuntu 18.06 Server with 8GB RAM and 2 vcpus, hosted by Microsoft Azure Services
- Free Google Colaboratory account with acces to NVIDIA graphics board
- C++ standard distribution for XCode (macOS Catalina 10.15.6).
- MATLAB License provided by Universidad Nacional de Colombia.
- Python 3.x.

## 11 Results

The object of study is a binary alloy with a bipartite lattice structure, in which the main interaction is due to atomic bonds. Heuristically, it is assumed that vacancies have a non zero interaction energy with atoms [4], this models local redistribution of charge and lattice vibrations. For clarity, vacancies are denoted as V type, and atoms by either A or B types. interaction energies are denoted

by  $\epsilon_{XY}$ , with  $X$  and  $Y$  denoting a particular type. Likewise, the total number of nearest neighbour bonds involving types  $X$  and  $Y$  is denoted by  $N_{XY}$ . Review the notation index at the beginning of the document.

## 11.1 SO1 - Derivation of Alloy Hamiltonian

Given that the aim of the project is to study the influence of vacant lattice sites on the equilibrium properties of a binary alloy, the following interaction Hamiltonian is considered

$$H = \epsilon_{AA}N_{AA} + \epsilon_{BB}N_{BB} + \epsilon_{AB}N_{AB} + \epsilon_{AV}N_{AV} + \epsilon_{BV}N_{BV} \quad (36)$$

Notice that a non zero bond energy between atoms and vacant sites is assumed. According to previous works on kinetics of ordering transitions in binary alloys, carried out by Porta, Frontera and others [19], this is a rather heuristic approach for taking into account lattice vibrations.

Since the lattice to be considered is assumed to be bipartite, there exist two sublattices whose sites are nearest neighbours to one another. Those sublattice are notated by  $A_2$  and  $B_2$ . Lattice variables are defined, on each sublattice, on equation 37. These set of variables allows description of the alloy alloy in terms of a ferromagnetic BEG Hamiltonian.

$$S_i^{(A_2)} = \begin{cases} 1 & \text{if site } i \text{ is occupied by an A-type atom} \\ 0 & \text{if site } i \text{ is vacant} \\ -1 & \text{if site } i \text{ is occupied by a B-type atom} \end{cases} \quad (37)$$

$$S_i^{(B_2)} = \begin{cases} 1 & \text{if site } i \text{ is occupied by an B-type atom} \\ 0 & \text{if site } i \text{ is vacant} \\ -1 & \text{if site } i \text{ is occupied by a A-type atom} \end{cases} \quad (38)$$

Notice that in terms of these variables

$$2N_{AA} = \sum_{i_{A_2}} \delta_{i,1}^{(A_2)} \sum_{i_{B_2}} \delta_{i,-1}^{(B_2)} \quad (39)$$

$$2N_{BB} = \sum_{i_{A_2}} \delta_{i,-1}^{(A_2)} \sum_{i_{B_2}} \delta_{i,1}^{(B_2)} \quad (40)$$

$$2N_{AB} = \sum_{i_{A_2}} \delta_{i,1}^{(A_2)} \sum_{i_{B_2}} \delta_{i,1}^{(B_2)} + \sum_{i_{A_2}} \delta_{i,-1}^{(A_2)} \sum_{i_{B_2}} \delta_{i,-1}^{(B_2)} \quad (41)$$

$$2N_{AV} = \sum_{i_{A_2}} \delta_{i,1}^{(A_2)} \sum_{i_{B_2}} \delta_{i,0}^{(B_2)} + \sum_{i_{A_2}} \delta_{i,0}^{(A_2)} \sum_{i_{B_2}} \delta_{i,-1}^{(B_2)} \quad (42)$$

$$2N_{BV} = \sum_{i_{A_2}} \delta_{i,-1}^{(A_2)} \sum_{i_{B_2}} \delta_{i,0}^{(B_2)} + \sum_{i_{A_2}} \delta_{i,0}^{(A_2)} \sum_{i_{B_2}} \delta_{i,1}^{(B_2)} \quad (43)$$

$$(44)$$

With

$$\delta_{i,1}^{(X)} = \frac{1}{2} S_i^{(X)} (S_i^{(X)} + 1) \quad (45)$$

$$\delta_{i,-1}^{(X)} = \frac{1}{2} S_i^{(X)} (S_i^{(X)} - 1) \quad (46)$$

$$\delta_{i,0}^{(X)} = 1 - (S_i^{(X)})^2 \quad (47)$$

In the appendix exact calculation of the Hamiltonian 36 in terms of lattice variables is performed. The result is quoted on equation 48, in the particular case when the atom vacancy interaction is independent of the atom type.

$$H = -\frac{J}{2} \sum_{\langle i_{A_2}, j_{B_2} \rangle} S_{i_{A_2}} S_{j_{B_2}} + \frac{K}{2} \sum_{\langle i_{A_2}, j_{B_2} \rangle} S_{i_{A_2}}^2 S_{j_{B_2}}^2 + D \sum_i S_i^2 \quad (48)$$

And

$$J = \frac{1}{4} (\epsilon_{AA} + \epsilon_{BB} - 2\epsilon_{AB})$$

From discussion of section 2.1,  $J > 0$  implies ordering similar to  $\beta$ -brass. It has thus been proven that the alloy Hamiltonian is equivalent to a BEG ferromagnetic Hamiltonian. Although Porta and Castán use an antiferromagnetic Hamiltonian to study ordering transitions in binary alloys [22], the equivalence with a ferromagnetic Hamiltonian is readily established by the symmetry of sublattice spin flipping present in both BEG and Ising Models defined on bipartite lattices **Cite Someone**.

Since the aim of the project is study of order-disorder transitions in a binary alloy, first order transitions will not be considered in this project. Second order transitions for Hamiltonian 48 are characterised by the order parameter

$$m = \langle S_i^{(A_2)} \rangle + \langle S_i^{(B_2)} \rangle \quad (49)$$

From the work of Wang and others, second order phase transitions may occur in a parameter range  $J + K < 0$  and  $D < 0$  [24]. These are characterised by order parameter

$$Q = \langle (S_i^{(A_2)})^2 \rangle - \langle (S_i^{(B_2)})^2 \rangle \quad (50)$$

However, given the constraint imposed on  $J$  by the requirement that there be an ordering transitions as described on section 2.1 is inconsistent with staggered quadrupolar ordering as described by Wang [24]. Therefore, the only relevant order parameter for the phase transitions studied in this project is

$$m = \langle S_{i_{A_2}} \rangle + \langle S_{i_{B_2}} \rangle \quad (51)$$

## 11.2 SO2 - Landau Theory for BEG Hamiltonian

Given that the system is constrained by particle concentration, statistical mechanical analysis in the canonical ensemble is quite involved. Therefore, it is wiser to resort to an analysis in the grand

canonical ensemble. This amounts to performing a Legendre transformation of the Hamiltonian of the form

$$H \rightarrow H - (\mu_V - \mu_B)N_V - (\mu_A - \mu_B)N_A \quad (52)$$

By noticing that

$$N_A = \sum_{i_A} \delta_{i,1}^{(A)} + \sum_{i_B} \delta_{i,-1}^{(B)} \quad (53)$$

$$N_V = \sum_i (1 - S_i^2) \quad (54)$$

It is clear that the transformation leads to a Hamiltonian of the form

$$H = H = -\frac{J}{2} \sum_{\langle i_{A_2}, j_{B_2} \rangle} S_{i_{A_2}} S_{j_{B_2}} + \frac{K}{2} \sum_{\langle i_{A_2}, j_{B_2} \rangle} S_{i_{A_2}}^2 S_{j_{B_2}}^2 + \mu \sum_i S_i^2 + h \sum_{i_B} S_{i_B} - h \sum_{i_A} S_{i_A} \quad (55)$$

With  $2h = \mu_A - \mu_B$ . Notice that in the case of a stoichiometric binary alloy, with equal concentration of each type of atoms, chemical potentials are equal, and thus  $h = 0$ . If  $h \rightarrow -\infty$ , the alloy is composed only of type A atoms. On the other hand, if  $h \rightarrow \infty$ , the alloy is composed only of B type atoms. By the same token, the limit  $\mu \rightarrow -\infty$  is akin to an alloy without vacant lattice sites. From now on, the reader might reckon that  $h$  is equivalent to a staggered external magnetic field, and  $\mu$  is an anisotropy term, pretty much as if the system were a magnetic solid [4].

Hamiltonian 55 has already been studied by Blume, Emery and Griffiths, in the absence of staggered external field[4]. Their work showed that there is a tricritical point at

$$\begin{aligned} k_B T_c &= \frac{1}{3} J z \\ \mu_c &= \frac{2}{3} \ln(2) J z \\ h &= 0 \end{aligned}$$

For  $K = 0$  [4]. Notice, however, that such a high value for  $\mu$  is inconsistent with the objective of studying phase transitions at low vacancy concentration. Therefore, multicriticality is not expected to be a part of the project's concerns, in principle. Although Porta, Frontera and others [19] emphasize that the condition  $K = 0$  alters significantly the kinetics of domain formation in binary alloys; considering the Landau theory for a Hamiltonian with  $K \neq 0$  in the presence of an staggered field is quite intricate. Furthermore, the work of Blume, Emery and Griffiths show that equilibrium properties in the case  $K \neq 0$ , although quantitatively different, is not qualitatively different to the case  $K = 0$  in a certain range [4]. In consequence, and as a first approximation, only the case  $K = 0$  is considered in the present project.

Consider the simplified Hamiltonian

$$H = -\frac{J}{2} \sum_{\langle i_{A_2}, j_{B_2} \rangle} S_{i_{A_2}} S_{j_{B_2}} + \mu \sum_i S_i^2 + h \sum_{i_B} S_{i_B} - h \sum_{i_A} S_{i_A} \quad (56)$$

Defined on a bipartite lattice. The following variational Hamiltonian is proposed

$$\hat{H} = -\gamma_A \sum_{i_{A_2}} S_{i_{A_2}} - \gamma_B \sum_{i_{B_2}} S_{i_{B_2}} + \mu \sum_i S_i^2 \quad (57)$$

The partition function for the variational Hamiltonian 57 is

$$\hat{Z} = Z_{A_2}^{N/2} Z_{B_2}^{N/2} \quad (58)$$

With

$$Z_{A_2} = 1 + 2e^{-\beta\mu} \cosh(\beta\gamma_A) \quad (59)$$

$$Z_{B_2} = 1 + 2e^{-\beta\mu} \cosh(\beta\gamma_B) \quad (60)$$

Variational free energy is computed easily. By defining  $m_A = \langle S_{i_A} \rangle$  and  $m_B = \langle S_{i_B} \rangle$ , it is straight forward to note that variational free energy, according to GBF method, is

$$\frac{\hat{F}}{N} = m_A \left[ \frac{\gamma_A}{2} - \frac{Jz}{4} m_B - \frac{h}{2} \right] + m_B \left[ \frac{\gamma_B}{2} - \frac{Jz}{4} m_A + \frac{h}{2} \right] - \frac{1}{2\beta} \ln Z_{A_2} - \frac{1}{2\beta} \ln Z_{B_2} \quad (61)$$

Also

$$m_A = \frac{1}{\beta} \frac{\partial \gamma_A}{\partial \ln Z_A} \quad (62)$$

$$m_B = \frac{1}{\beta} \frac{\partial \gamma_B}{\partial \ln Z_B} \quad (63)$$

Minimisation of variational free energy with respect to parameters  $\gamma_A$  and  $\gamma_B$  thus lead to the conditions

$$\gamma_A = Jzm_B + h \quad (64)$$

$$\gamma_B = Jzm_A - h \quad (65)$$

For simplicity, the unit of energy is chosen as  $Jz$ ,  $z$  being the coordination number of the lattice, and the unit of entropy is taken as  $k_B$ . The system of equations 63 may be rewritten as

$$m_A = f(m_B + h) \quad (66)$$

$$m_B = f(m_A - h) \quad (67)$$

With

$$f(u) = \frac{2 \sinh(\beta u)}{e^{\beta\mu} + 2 \cosh(\beta u)} \quad (68)$$

Notice that the order parameter of the transitions

$$m = m_A + m_B$$

Also, a rather simple solution is intuted by the parity of  $f(u)$ :  $m_A = -m_B$ . The following change of variables is made

$$m_A = m + n$$

$$m_B = m - n$$

And thus the system of equations 67 amounts to

$$m + n = f(m + (h - n)) \quad (69)$$

$$m - n = f(m - (h - n)) \quad (70)$$

A rather simple solution is readily seen

$$m = 0 \quad (71)$$

$$n = n_0 = f(h - n_0) \quad (72)$$

In general, the system of equations 70 amounts to

$$m = \frac{1}{2} \left[ f(m + (h - n)) + f(m - (h - n)) \right] \quad (73)$$

$$n = \frac{1}{2} \left[ f(m + (h - n)) - f(m - (h - n)) \right] \quad (74)$$

$$(75)$$

The simple solution presented before is valid in the disordered phase of the alloy. A solution with non zero order parameter corresponds to an ordered phase of the alloy. Near a critical point, approaching from the disordered phase, the first equation of system 75 is equivalent to

$$m = f'(h - n)|_{n=n_0} m + \mathcal{O}(m^2) \quad (76)$$

This equation has non trivial solution only if

$$f'(h - n)|_{n=n_0} > 1 \quad (77)$$

The boundary for second order transitions is thus given by

$$f'(h - n)|_{n=n_0} = 1 \quad (78)$$

This criterion can be derived by expanding variational free energy near  $m = 0$ , and imposing the condition

$$\frac{\partial^2 \hat{F}}{\partial m^2} = 0$$

A condition that is an elementary consequence of mathematical analysis. As a reminder, at critical point, the only absolute minimum of variational energy is  $m = 0$ . Given the symmetry of the Hamiltonian upon global spin flip, the variational energy is expected to be an even function of order parameter. Therefore, the condition for the existence of a non zero value of magnetisation is

$$\frac{\partial^2 \hat{F}}{\partial m^2} < 0$$

And the boundary of phase transitions thus lies in the surface that satisfies the stated criterion. A proof that the both stated criteria are equivalent is rather lengthy and is not stated explicitly. This proof would be quite illustrative if first order transitions were considered, and multicriticality an object of this project. For, then, a criterion o the fourth derivative of the free energy with respect to order parameter would yield the value of the tricritical point of the system [4, 25]. Since this project is concerned only with second order transitions, the criterion 78 is enough.

In this mean field approximation, order parameter profiles as a function of temperature (for given  $\mu$  and  $h$ ) should be computed numerically. Clearly, for a given  $\mu$ , the critical curve on  $h - T$  plane should also be computed numerically. A limit case can be readily identified, though. In the limit of zero vacancy concentration,  $\mu \rightarrow -\infty$ , the system of consistency equations 75 is clearly identical to that derived by Porta and Castán [22]. Therefore, at least from Landau theory, it can be concluded that a spin-1/2 Ising Model can be used to describe ordering transitions of binary alloys, in the limit of very low vacancy concentration. As will be shown, Landau Theory predicts that at higher vacancy concentrations, the results are qualitatively similar to those derived by Porta and Castán [22].

### 11.3 Numerical Computations of Mean Field Curves

Before presenting numerical results concerning magnetisation profiles and critical curves, it is healthy to study limit cases. The limit  $h = 0$  was studied by Blume, Emery and Griffiths [4]. They proved that, in the limit of very low vacancy concentration, the critical temperature is  $T_c = 1$ . Also, critical temperature is related to  $\mu$  by

$$\mu_c = T_c \ln \left[ 2 \frac{1 - T_c}{T_c} \right] \quad (79)$$

From this equation it is clear that large changes in chemical potential  $\mu$  do not produce a dramatic change of critical temperature. And thus, it can be expected that the results obtained by Porta and Castán [22] are of very general qualitative value even for non-negligible vacancy concentration.

On the other hand, at  $T_c = 0$ , the energy of the ground state is equal to

$$E_m = -\frac{N}{2} + \mu N$$

If the external field is such that  $h = 1$ , the staggered configuration, i.e. with A-B bonds, has an energy

$$E_m = -\frac{N}{2} + \mu N$$

And thus the lowest energy level is degenerate. At higher values of the external field, the staggered configuration has lower energy than the parallel-spin configuration. And then, at  $h = 1$  there is a transition from parallel-spin configuration to staggered spin configuration. Therefore, this should be a critical point on the critical curve on  $h - T$  plane for second order phase transitions.

### 11.3.1 Numerical Results of Mean Field Magnetisation

From the set of consistency equations 63, magnetisation as a function of temperature, for fixed negative  $\mu$ , at  $h = 0$  was computed. The results are presented on figure 11.3.1. Notice that all the curves are qualitatively similar, except for the fact that, for relatively high vacancy concentration, the critical temperature is shifted towards  $T = 1/3$ , whereas for very low vacancy concentration, the critical temperature is shifted towards  $T = 1$ . This is in agreement with Blume, Emery and Griffiths' results [4]. A quite important feature, that will be explicitly shown, is that for a high enough external field <sup>2</sup>, the system returns to a zero order parameter state at low temperature. This is a direct consequence of the degeneracy of the lowest energy level discussed before. If the external field, at low vacancy concentration, is larger than 1.2 approximately, there is no second order phase transition characterised by order parameter  $m$ . In fact, it is expected that at very high external fields, the ordering is staggered <sup>3</sup>.

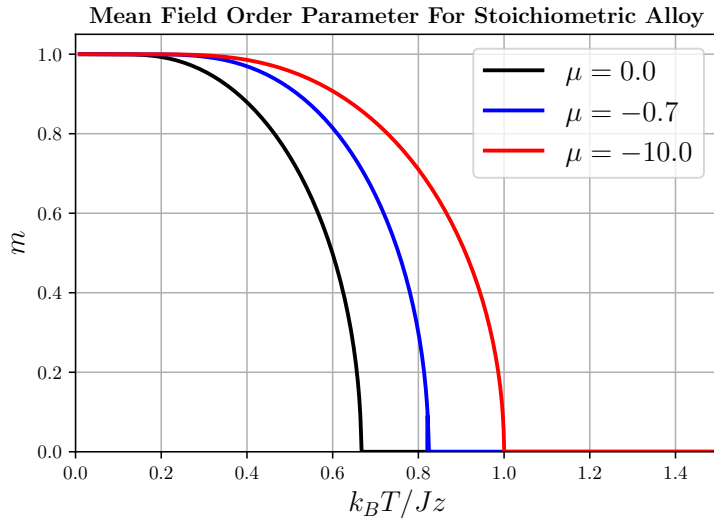


Figure 6: Temperature profile of order parameter, for a stoichiometric binary alloy, for different values of vacancy chemical potential. The more negative the chemical potential, the smaller the vacancy concentration.

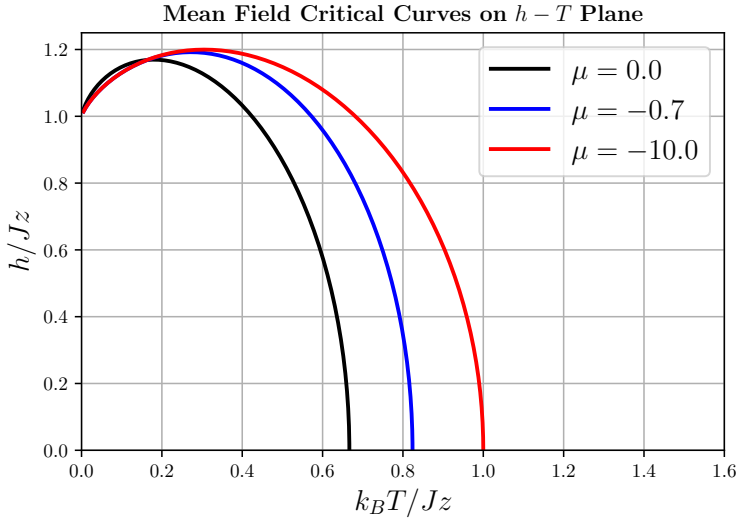


Figure 7: Critical curves on  $h - T$  plane, in the mean field approximation. The more negative the chemical potential, the smaller the vacancy concentration.

### 11.3.2 Numerical Calculations of Critical Curves on $h - T$ and $x - T$ Planes

The critical curve in the  $h - T$  plane for constant negative  $\mu$  is presented in figure 11.3.2. The limit cases discussed before are present, and the figure shows that the curves vary qualitatively rather than quantitatively as  $\mu$  is varied. Therefore, the intuition that Porta and Castán's results [22] might be of general validity even for finite vacancy concentrations seems to be confirmed.

Notice that the critical curve has a global maximum, and is concave downwards. This explains why for high enough external field, there is a low temperature below which the order parameter vanishes. On the region above the curve, order parameter is zero. Immediately below the curve, order parameter is finite. As mentioned before, the nature of this curve is due to the fact that a high external field lowers the energy of the staggered state.

Computation of the critical curve in  $x - T$  space for fixed negative  $\mu$  requires computation of

$$n = \frac{m_A - m_B}{2} = \frac{N_A - N_B}{N} \approx 2x - 1$$

At the critical curve on  $h - T$  plane. The results are shown on figure 11.3.2. Compare to those on figure 3. Notice that these curves are very similar to those reported by Porta and Castán [22]. At zero external field, critical concentration is  $x_c = 0.5$ , as is expected. On the other hand, critical concentration at  $T_c = 0$  is  $x_c = 1$ , which is consistent with the staggered nature of the ground state.

---

<sup>2</sup>either positive or negative due to the spin flipping symmetry of the Hamiltonian

<sup>3</sup>Bonds A-A or B-B are preferred rather than A-B

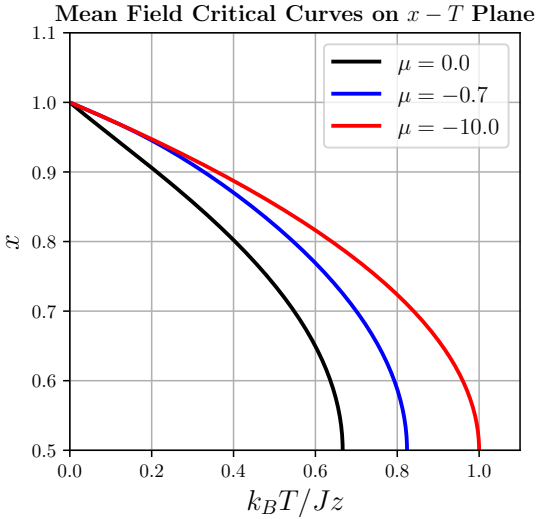


Figure 8: Temperature profile of order parameter, for a stoichiometric binary alloy, for different values of vacancy chemical potential. The more negative the chemical potential, the smaller the vacancy concentration.

#### 11.4 SO3 - Computation of Thermodynamic Quantities using Markov Chain Monte Carlo

The Hamiltonian 56 was sampled using Metropolis Algorithm, thus following Glauber dynamics. The exchange integral  $J = 1$ , and units of entropy were taken as  $k_B$ . Due to time constraints, the following values for the external fields, related to chemical potential difference, were used:

$$\mu = 0.0, -1.7 \quad (80)$$

$$h = 0.0, 0.1, 0.3, 0.5 \quad (81)$$

In figure 9, order parameter, internal energy, specific heat and order parameter derivative are presented for  $\mu = 0.0$ ,  $h = 0.0$  and  $\mu = 0.0$ ,  $h = 0.5$ <sup>4</sup>. As can be seen in the figure, a stoichiometric binary alloy presents a quite sharp second order transition near a critical temperature  $T_C = 0.809$ . In contrast, a non-stoichiometric alloy presents a rather weak peak near an inflection temperature  $T_C = 1.496$ . This is striking, specially when compared to the mean field approximation. It will be shown later that stoichiometric and non-stoichiometric alloys present quite different scaling with lattice size. Although computation of thermodynamic quantities is explicitly shown only for a pair of points  $(\mu, h)$ , this tendency is present for all values of  $\mu$  and  $h$ , as can be seen by the order parameter profiles presented on figures 10 and 11<sup>5</sup>.

<sup>4</sup>Simulations corresponds to a lattice size  $L = 16$ .

<sup>5</sup>The programs used for data generation are introduced on the appendix.

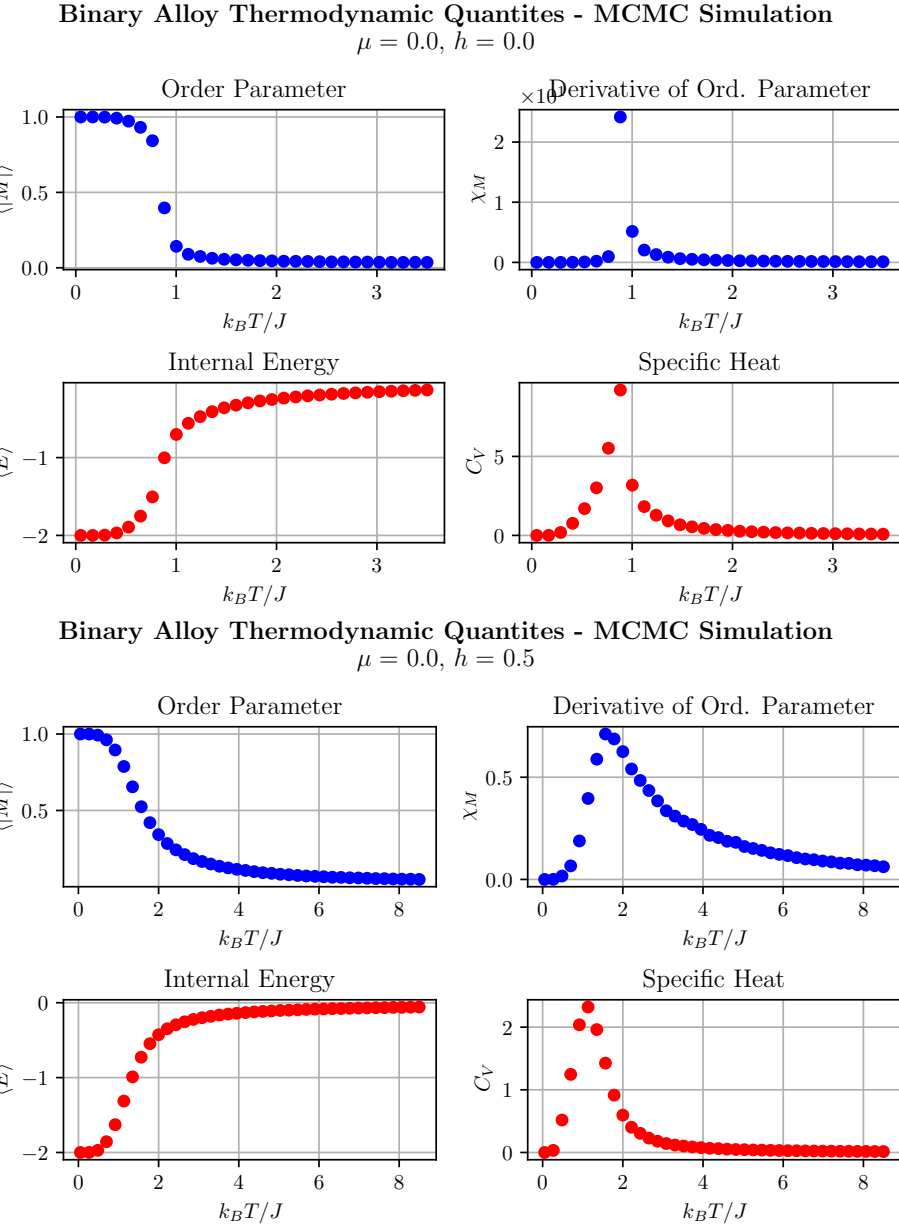


Figure 9: Thermodynamic quantities of Binary Alloy for a fixed vacancy chemical potential  $\mu = 0.0$ . Stoichiometric alloy,  $h = 0.0$ , presents a clearly visible critical point at  $T_C = 0.809$ . Non stoichiometric binary alloy,  $h = 0.5$ , does not present such a sharp transition; an inflection point, which coincides with maximum of order parameter derivative, is present at  $T_C = 1.496$ .

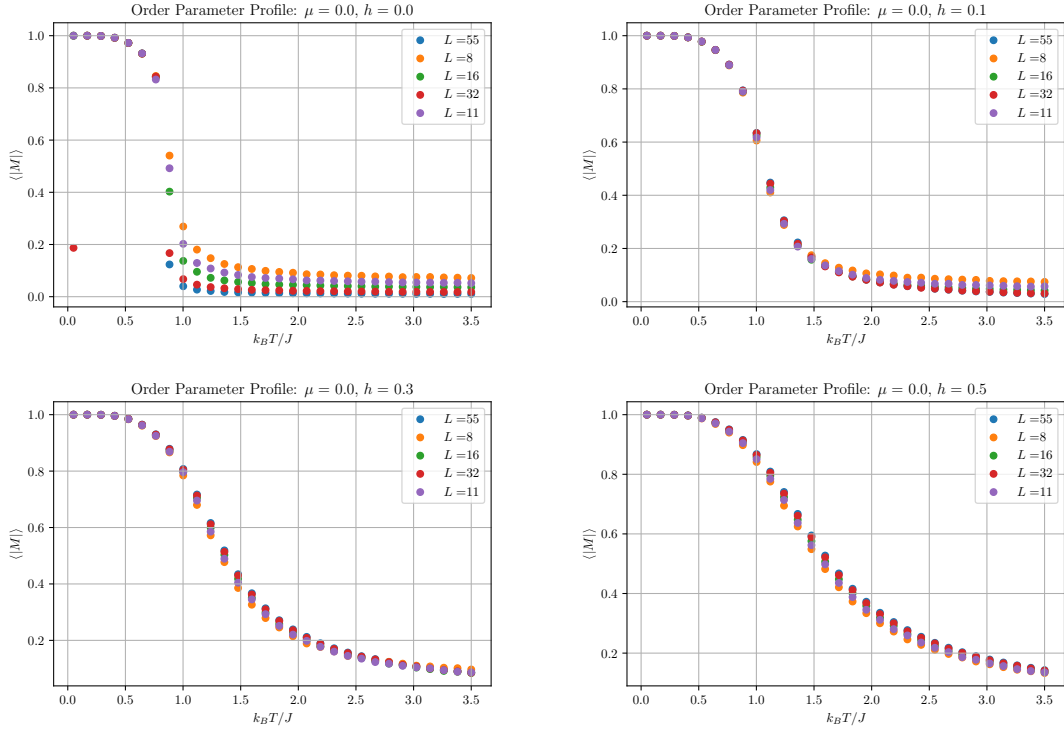


Figure 10: Order parameter profiles for several values of  $h$  and lattice sizes  $L$ , with  $\mu = 0$ . Notice how stoichiometric alloy has a different lattice size scaling than non-stoichiometric alloys. Critical temperature for stoichiometric alloy, and inflection temperature for non-stoichiometric alloys, are determined using the method posed by Ibarra and others [12].

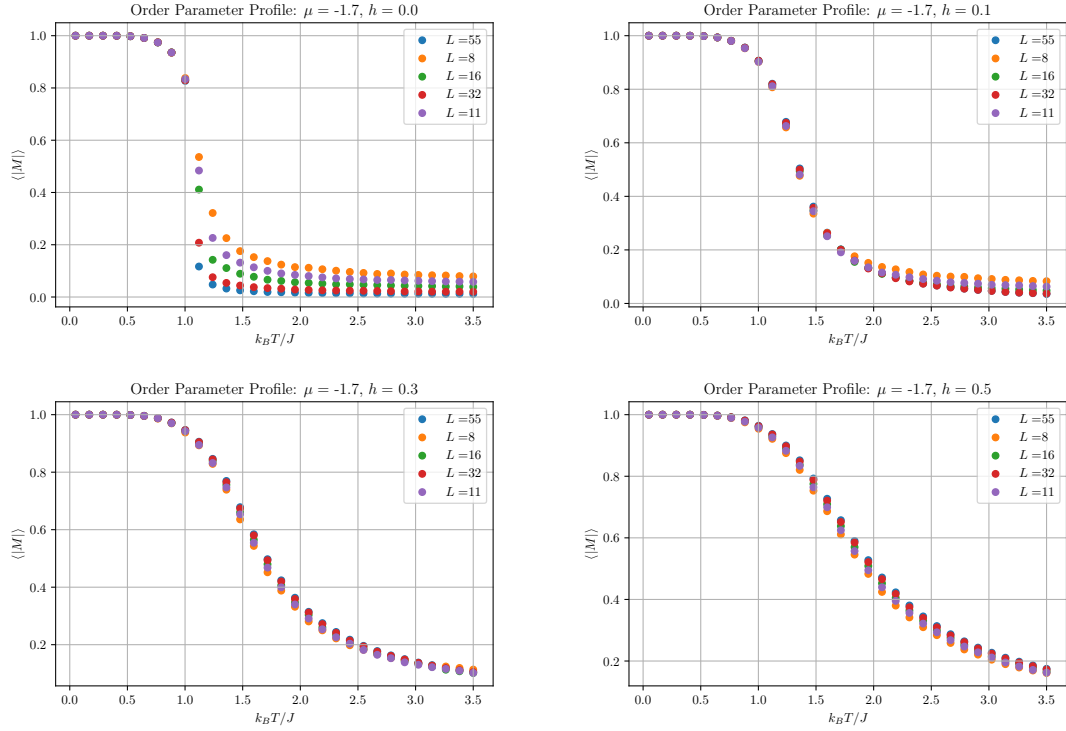


Figure 11: Order parameter profiles for several values of  $h$  and lattice sizes  $L$ , with  $\mu = -1.7$ . Notice how stoichiometric alloy has a different lattice size scaling than non-stoichiometric alloys. Critical temperature for stoichiometric alloy, and inflection temperature for non-stoichiometric alloys, are determined using the method posed by Ibarra and others [12].

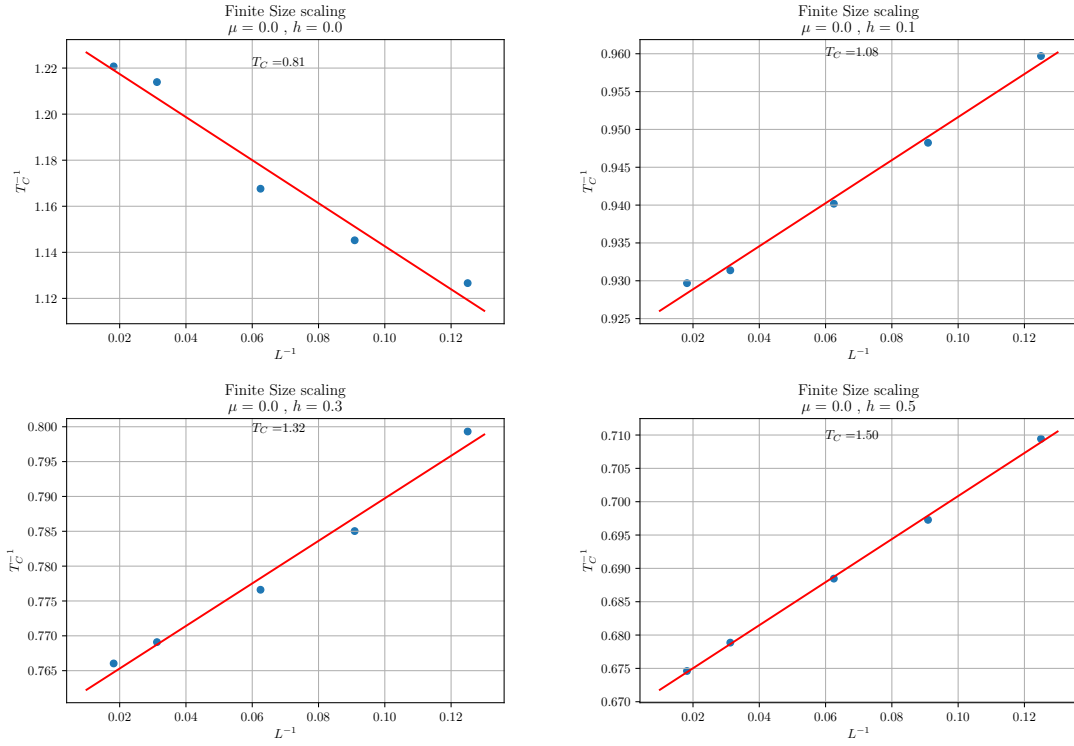


Figure 12: Finite size scaling following Ibarra and others for several values of  $h$ , with  $\mu = 0.0$ . Notice how stoichiometric alloy has a different lattice size scaling than non-stoichiometric alloys. Critical temperature for stoichiometric alloy, and inflection temperature for non-stoichiometric alloys, are determined by the inverse of the intercept of linear fits [12].

### 11.5 SO4 - Computation of Critical Points on $h - T$ Plane

Details of the application of Ibarra and others' method for computing critical temperature in the thermodynamic limit  $L \rightarrow \infty$  are left to the appendix. It is based on the computation of the inflection point of order parameter profiles (figures 10 and 11) for all lattice size considered ( $L = 8, 11, 16, 32, 55$ ). Plots of inflection temperature  $T_c$  as a function of lattice size are presented on figures 12 and 13. Notice how scaling with size is different for stoichiometric alloys and non stoichiometric alloys. For stoichiometric ones, inflection temperature diminishes as lattice size increases. The opposite is true for non stoichiometric alloys.

Due to time constraints, only 8 critical temperatures were computed: 4 corresponding to  $\mu = 0.0$ , and 4, to  $\mu = -1.7$ . These were calculated from the intercept of linear fits in figures 10 and 11. Results are summarised on tables 3 and 4.

Unfortunately, not enough inflection points were computed in order to be able to interpolate a critical curve on  $h - T$  plane

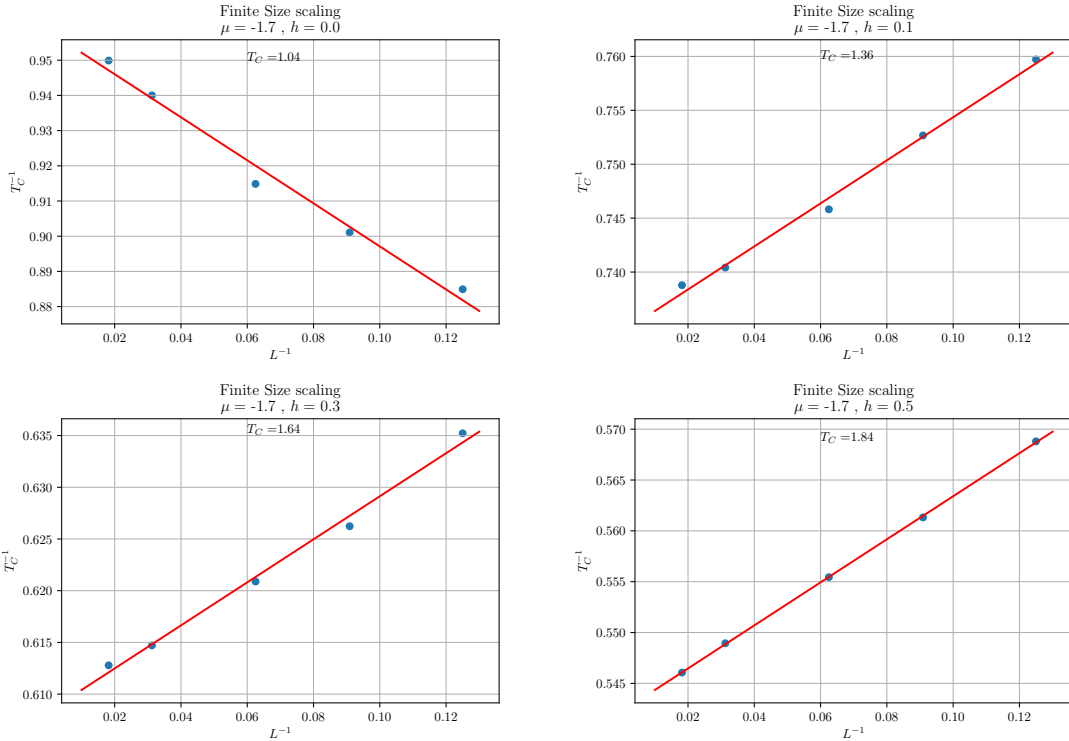


Figure 13: Finite size scaling following Ibarra and others for several values of  $h$ , with  $\mu = -1.7$ . Notice how stoichiometric alloy has a different lattice size scaling than non-stoichiometric alloys. Critical temperature for stoichiometric alloy, and inflection temperature for non-stoichiometric alloys, are determined by the inverse of the intercept of linear fits [12].

$h/J$	$k_B T_C/J$
0.0	0.809
0.1	1.083
0.2	1.317
0.3	1.496

Table 3: Inflection temperatures for  $\mu = 0.0$ . Notice that inflection temperature increases with  $h$ , i.e. when atom concentration favours either type A or type B atoms.

$h/J$	$k_B T_C/J$
0.0	1.044
0.1	1.362
0.2	1.644
0.3	1.844

Table 4: Inflection temperatures for  $\mu = 0.0$ . Notice that inflection temperature increases with  $h$ , i.e. when atom concentration favours either type A or type B atoms. Also notice that inflection temperatures are higher than those obtained by setting  $\mu = 0.0$ .

## 12 Discussion

From the previous sections, it has been demonstrated that a BEG Hamiltonian can be used to describe order transitions in substitutional binary alloys. Results are compared to those obtained by Porta and Castán [22].

### 12.1 SO1 - BEG Hamiltonian for Substitutional Binary Alloys

Calculations taking into account only atom bond energies have been proved to lead to a ferromagnetic BEG Model. Although Porta and Castán consider an antiferromagnetic model, in the absence of an external field, the symmetry of Ising-like models under sublattice spin flipping implies that ferromagnetic and antiferromagnetic models (in the absence of external field) are equivalent by the definition of lattice site variables like on equation 37. Therefore, the usage of a ferromagnetic Hamiltonian rather than an antiferromagnetic Hamiltonian is a matter of convenience.

In the presence of an external field, the ferromagnetic Hamiltonian loses its symmetry. However, ferromagnetic Hamiltonian retains its symmetry if the field in question is staggered. This motivates the mapping of the interaction Hamiltonian from an antiferromagnetic one, to a ferromagnetic in the presence of an staggered field. As was shown in section 11, statistical analysis in the grand canonical ensemble leads to a Hamiltonian in the presence of an staggered field. Therefore, the chosen Hamiltonian seems to be a perfectly good option in comparison to Porta and Castán antiferromagnetic one.

Of capital importance is the interaction constant  $K$ , since it tries to model lattice vibration as well as other global phenomena [19]. However, from Landau theory, analytical calculations are tremendously complicated, and only the case of a stoichiometric alloy, the results can be computed exactly [4, 19]. Therefore, as a first approximation, it seems necessary to neglect this constant, since the inclusion of a staggered field is of huge importance for the study of the influence of atom concentration on the ordering transitions in substitutional binary alloys.

## 12.2 SO2 - Landau Theory for BEG Alloy Hamiltonian

A very general expression for the critical curve has been derived (78), that is consistent with Porta and Castán's results in the limit of very low vacancy concentration ( $\mu \rightarrow -\infty$ ). This is a quite remarkable result, since it seems to imply that the spin-1/2 Ising Model can be used to accurately describe substitutional binary alloys, even in the presence of a finite impurity concentration. Conclusions are however limited by the constraint  $K = 0$ . Also, as pointed out by Porta, Vives and others [19], an asymmetry term on the Hamiltonian should be included to account for global lattice phenomena.

From the perspective of Landau Theory, the mathematical treatment presented, although equivalent to that of Porta and Castán's, seems to be more explicit, in that it directly computes a variational free energy following GBF method, and demonstrates that the optimal variational parameters are related directly to the order parameter of the continuous phase transitions. Although a direct series expansion of the free energy is not carried out, the consistency equations 67 are solved to first order on the order parameter, thus leading to an explicit statement of the condition of an order transition: that there exists a non trivial minimum of the system's free energy.

Although not explicitly shown, the symmetry of the Hamiltonian under lattice spin flip implies that the free energy is an even function of the order parameter. It would be a quite interesting matter to show this explicitly by performing a series expansion at  $m = 0$ . The mathematical complexity is quite restrictive, though. Besides, a complete series expansion of free energy at  $m = 0$  is of practical importance if multicritical phenomena is to be studied, hence, it is not carried out beyond second order in this project.

### 12.2.1 Comparison of Numerical Mean Field Calculations

A remarkable feature of the numerical results obtained regarding Landau Theory is that the results are qualitatively similar to those obtained by Porta and Castán [22]. This seems to imply that a spin-1/2 Ising-like Model may be used to describe qualitatively ordering transitions in substitutional binary alloys, even for non-zero vacancy concentration. However, conclusion in this direction are limited due to the assumption  $K = 0$  which was discussed before.

A quite interesting feature is the staggered ordering that appears when the external field is larger than 1.2 approximately. It has been shown that this is a direct consequence of the degeneracy of the lowest energy level of the system at  $T_c = 0$ . This result is of limited validity, since high enough concentrations might imply changes in the lattice structure <sup>6</sup> that completely affect the consequences of the model, which is based upon the assumption that the lattice is bipartite.

## 12.3 SO3 - Computation of Thermodynamic Quantities via Markov Chain Monte Carlo

As pointed out in section 14.2.1, the numerical routines implemented might be biased due to human error, in the case of non stoichiometric binary alloys. Stoichiometric binary alloys, however, seem to agree qualitatively with mean field approximations in the sense that increasing vacancy concentration implies a decrease of critical temperature (see figure 11.3.2, and compare with tables 3 and 4, with  $h = 0$ ). As expected, though, mean field calculations are not completely reliable, since fluctuations in order parameter are neglected. A quite important result is the computation

---

<sup>6</sup>This is pointed out by [10]

of critical temperatures using Ibarra and others' method [12]. As is shown in figures 12 and 13, inflection temperatures follow a remarkable linear relation, which is consistent with the size scaling of Ibarra and others.

Returning to non-stoichiometric alloys, although a peak in both specific heat and order parameter derivative is present at an inflection temperature, it is not as sharp as those of stoichiometric alloys. As a matter of fact, ordering appears to occur smoothly, since size scaling does not seem to be a very important factor, as shown on figures 10 and 11. Size scaling arises due to limitation on correlation length when considering a finite system. In the thermodynamic limit, correlation length is infinite [17, 12, 15], while finite systems can only have a correlation length that is at most as large as its characteristic linear dimension. The particular scaling demonstrated by non-stoichiometric alloys, as shown on figures 12 and 13, seems to contradict this picture of a discontinuous ordering transition.

#### 12.4 SO4 - Comparison of Critical Points Obtained Using MCMC and Mean Field Approximation

Due to time constraints, caused by failures of the hardware used in the computation of MCMC data (see 10), a complete critical curve on  $h-T$  plane could not be obtained. As pointed out in the previous section, however, stoichiometric alloys agree qualitatively with Mean Field approximation calculations. Critical temperature depends mainly on the value of exchange integral  $J$ , which might be fitted to experimental data to determine the validity of the Hamiltonian 56 for modelling ordering phenomena in substitutional alloys. A quite important result of the model is that, at least for stoichiometric alloys, critical temperature can be determined for different vacancy concentrations, showing that increasing vacancy concentration implies lower critical temperature. This is expected due to the exponential increase on the number of available microstates consistent with a given macrostate that comes with the usage of a Spin-1 Model.

Although the results related to non-stoichiometric alloys require a thorough review, MCMC simulations seem to demonstrate that vacancy dynamics is a phenomenon of capital importance in the computation of equilibrium properties of substitutional alloys. As is illustrated on figure 14, vacancies interact strongly with domain borders. This means that vacancy diffusion is a key phenomenon that determines not only the kinetics of the thermalisation process, but also equilibrium properties of a substitutional binary alloy.

### 13 Conclusions

It has been proven that a substitutional binary alloy in which the main contribution to the interaction energy are atomic bounds, can be mapped to a ferromagnetic BEG Hamiltonian, which in turn can be mapped to an antiferromagnetic BEG Hamiltonian by the symmetry of lattice spin flip. Landau Theory was considered in order to characterise ordering phase transitions on a mean field approximation. A closed expression for the boundary of phase transition was found that agrees with previous results from both Porta and Castán, and Blume, Emery and Griffiths [22, 4]. Nonetheless, the results are to be taken with reserve, since it was assumed that  $K = 0$ , something that might be at odds with the kinetics of vacancy diffusion, according to Porta, Vives and others [19]. Numerical simulations are needed to confirm the conclusions drawn from Landau Theory.

As a matter of fact, this model can be further generalised to model more complex phenomena, like the effects of doping in ordering transitions. This can be done by setting  $K \neq 0$  [19]. Although

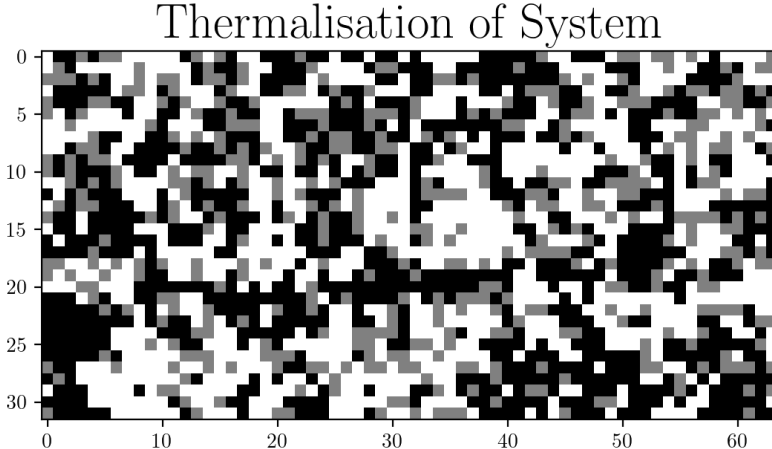


Figure 14: Alloy Thermalisation simulated using MCMC.  $A$  type atoms are represented by black sites,  $B$  type, by white sites, and vacancies by gray sites. Notice that vacancies tend to interact strongly with domain borders.

analytical calculations, even in the context of a mean field theory, can be quite involved, at least numerical approximations can be drawn from Landau Theory that could lead to a qualitative understanding. These calculations are of great relevance at low temperatures, where fluctuations are less important [17, 25].

Considering the work of Porta and Castán, this project constitutes a generalisation of the common Spin-1/2 Model for binary alloys that allows accounting for vacancy diffusion phenomena. This work is a step towards a model that may even account for impurities or lattice vibrations in the ordering of binary alloys. Not only is it possible to recover their results in the limit of very low vacancy concentration, but also critical temperature can be determined for non-zero vacancy concentration. It has been shown that lowering vacancy concentration increases critical temperature, with an upper limit set by the critical temperature of a Spin-1/2 Ising Model. With respect to Ibarra's work, the techniques developed for the study of magnetic systems have been extrapolated to the study of binary alloys. Not only has this project shown that Ising like models can be applied to non-magnetic systems, but also, has departed the common Spin-1/2 Ising Model to show that higher Spin models can be used to model systems with complex interactions between components of more than two species.

To the future, this project needs a thorough check of the size scaling of non-stoichiometric alloys in order to check the inflection temperatures reported on tables 3 and 4. More critical points need be computed to produce MCMC simulated critical curves that are closer to the actual thermal distribution of the system than mean field approximations. From a theoretical point of view, computations with  $K \neq 0$  should be carried out. Not only would this allow an heuristic account of lattice vibrations, according to Porta and Vives [19], but also would be an important step towards modelling the influence of impurities in the ordering phase transitions of binary alloys.

## 14 Appendix

This appendix contains the calculations related to specific objectives 1 and 2:

1. Explicit computation of BEG Hamiltonian parameters stated on equation 48.
2. Transcription of Google Colab Notebook used for numerical computation of critical curves.

### 14.1 Computation of BEG Hamiltonian

By expanding the kronecker deltas on equations 47, it is obtained that

$$N_{AA} = \frac{1}{8} \sum_{i_A, j_B} \left[ S_{i_A} S_{j_B} (S_{i_A} + 1)(S_{j_B} - 1) \right] \quad (82)$$

$$N_{BB} = \frac{1}{8} \sum_{i_A, j_B} \left[ S_{i_A} S_{j_B} (S_{i_A} - 1)(S_{j_B} + 1) \right] \quad (83)$$

$$N_{AB} = \frac{1}{8} \sum_{i_A, j_B} \left[ S_{i_A} S_{j_B} (S_{i_A} + 1)(S_{j_B} + 1) + S_{i_A} S_{j_B} (S_{i_A} - 1)(S_{j_B} - 1) \right] \quad (84)$$

$$N_{AV} = \frac{1}{8} \sum_{i_A, j_B} \left[ S_{i_A} (S_{i_A} + 1)(1 - S_{j_B}^2) + S_{j_B} (S_{j_B} - 1)(1 - S_{i_A}^2) \right] \quad (85)$$

$$N_{VA} = \frac{1}{8} \sum_{i_A, j_B} \left[ S_{i_A} (S_{i_A} - 1)(1 - S_{j_B}^2) + S_{j_B} (S_{j_B} + 1)(1 - S_{i_A}^2) \right] \quad (86)$$

By substituting these equations in Hamiltonian 36, and assuming that <sup>7</sup>

$$\epsilon_{AA} = \epsilon_{BB}$$

$$\epsilon_{AV} = \epsilon_{VA}$$

It is straightforward to see that the alloy Hamiltonian can be equivalent to a ferromagnetic BEG model with

$$\begin{aligned} J &= \frac{1}{4} \left( \epsilon_{AA} + \epsilon_{BB} - 2\epsilon_{AB} \right) \\ K &= \frac{1}{4} \left( \epsilon_{AA} + \epsilon_{BB} + 2\epsilon_{AB} - \epsilon_{AV} \right) \\ D &= \frac{z\epsilon_{AV}}{4} \end{aligned}$$

Notice that  $J$  determines the type of ordering. From considerations of section 2, it is clear that  $J > 0$ , and thus corresponds to a ferromagnetic BEG Hamiltonian. Notice that  $J$  is directly identifiable to the heat of solution of the alloy [6]. On the other hand, as pointed out by Porta, Vives and others,  $K$  is related to the interplay between atom bondas and those involving vacancies [19]. Here lies the fundamental reason why  $K = 0$  may be an over simplification. Finally,  $D$  is immaterial in the limits of low vacancy concentration.

---

<sup>7</sup>These assumptions are suggested by [19].

## 14.2 Python Codes For Markov Chain Monte Carlo Simulations

All codes are available on a public repository on Github under name [InvTeor](#), from user **diegoherera262**.

### 14.2.1 Fundamental Routines for Computing Thermodynamic Quantities

The following python code was used to simulate a centered rectangular binary alloy. It is listed as **IsingModel.py** on the project Github repository. Its core is a class called **IsingLattice2D**, which not only encodes a centered rectangular lattice in a 1D array, but also is capable of computing thermodynamic quantities after performing a MCMC step. It has as one of its properties, the values of the external fields  $\mu$  and  $h$ , as well as the lattice size. A lattice step consists of  $L^2$  single Monte Carlo Steps. All observables were computed after carrying out 15000 lattice Monte Carlo steps, sparing the first 5000.

**Important:** This program had an error on line 102: The staggered field did not cover the lattice correctly, for the lattice has  $2L^2$  sites and the line read

```
sig = -1 if idx >= self.LatticeSize else 1
```

This errata is corrected on the referenced version of this code, but not during simulations. This is a source of error that needs to be addressed when checking the results obtained in this project, specially regarding non-stoichiometric alloys.

```
import numpy as np
import random as rd
import matplotlib.pyplot as plt
import matplotlib.animation as animation
import time
from scipy.optimize import curve_fit

def num2bin(num):
    return [int(x) for x in '{0:02b}'.format(int(num))]

def MagsFit(x,A,B,C,D,E):
    return D*(np.tanh(A-B*x)+E)**C

class IsingLattice2D:

    '''Class For modelling an Ising Hamiltonian using Monte Carlo'''

    # Attributes of the class
    LatticeSize = 1
    NumSpins = 1
    Lattice = []
    Neighbours = None
    SpinflipKey = {
        -1:[0,1],
        0:[-1,1],
```

```

        1:[-1,0]
    }
mu = 0.0
h = 0.0

# Functions of the class

def __init__(self,LatticeSize = 16,mu = -1.0,h = 0.0):

    """
    Initialise Lattice with Random Integers -1,1
    """

    # Random initialization
    self.mu = mu
    self.h = h
    self.LatticeSize = LatticeSize
    self.NumSpins = 2*LatticeSize**2
    self.Lattice = [rd.choice([-1, 0, 1]) for x in range(self.NumSpins)]


def lidx2ij(self,lidx):

    """
    Function that converts linear array idx to 2D idx
    with Periodic Boundary Conditions
    """

    return np.array([(lidx//self.LatticeSize)%self.LatticeSize,\n                    lidx%self.LatticeSize])


def ij2lidx(self, idx_list):

    """
    Function that converts 2D idx to linear array idx
    with Periodic Boundary Conditions
    """

    return self.LatticeSize*(idx_list[0]%self.LatticeSize) + \
           idx_list[1]%self.LatticeSize


def cell(self, lidx):

    """
    Function that returns linear idx of numerated cells
    """

```

```

idx2d = np.array(self.lidx2ij(lidx))
return np.array([self.ij2lidx(np.add(idx2d,np.array(num2bin(k))))]\ 
for k in range(4)])

def FillNeighbours(self):
    """
    Function that fills array of neighbours for each S sublattice
    """

    auxcont = np.array([[self.cell(\ 
        self.ij2lidx(self.lidx2ij(idx) - k*np.array([1,1])))\ 
    for idx in range(self.LatticeSize**2)]\ 
    for k in range(2)])\ 

    dictLattice0 = {k:(auxcont[0,k]+self.NumSpins//2)\ 
        for k in range(self.NumSpins//2)}
    dictLattice1 = {(k+self.NumSpins//2):auxcont[1,k]\ 
        for k in range(self.NumSpins//2)}
    dictLattice0.update(dictLattice1)
    self.Neighbours = dictLattice0

def DeltaEnergy(self,next_spin,idx):
    """
    Compute energy difference for flipping.
    """

    dS = next_spin - self.Lattice[idx]
    s = next_spin + self.Lattice[idx]
    sig = -1 if idx >= self.LatticeSize**2 else 1
    return dS*(-0.5*sum(self.Lattice[k] for k in self.Neighbours[idx])+\ 
        self.h*sig + self.mu*s)

def MCStep(self,beta):
    """
    Implementation of a Monte Carlo Step.
    """

    # Choose random lattice site
    k = rd.randint(0,self.NumSpins-1)
    # Choose random new spin value
    flip_idx = 1
    if rd.uniform(0.0,1.0) < 0.5:
        flip_idx = 0

```

```

newspin = self.SpinflipKey[self.Lattice[k]][flip_idx]
# Accept according to Monte Carlo
if rd.uniform(0.0,1.0) < np.exp(-beta*self.DeltaEnergy(newspin,k)):
    self.Lattice[k] = newspin

# Compute statistically important quantities
def ConfigMagnetisation(self):

    """
    Compute Magnetisation of system
    """

    return sum(self.Lattice[k] for k in range(self.NumSpins))

def ConfigEnergy(self):

    """
    Compute Energy of system
    """

    return sum(self.Lattice[k]*(\
        -1.0*sum(self.Lattice[j] for j in self.Neighbours[k]) \
        + self.h\
        + self.mu * self.Lattice[k])
        for k in range(self.NumSpins//2)) + \
    sum(self.Lattice[k]*(-self.h + self.mu*self.Lattice[k])\
        for k in range(self.NumSpins//2,self.NumSpins))

def ConfigStatQuantities(self):

    """
    Compute Magnetisation & Energy of system
    """

    Eint = self.ConfigEnergy()
    M = np.abs(self.ConfigMagnetisation())
    return Eint, M

# Implement Lattice Monte Carlo Step
def LatticeMCStep(self,beta):

    """
    Implementation of a Monte Carlo Step on the lattice. This normalises
    execution time.
    """

```

```

    for step in range(0,self.NumSpins):
        self.MCStep(beta)

    # Perform simulation over temperature range
    def MCSimulation(\n
        self,Tmin=0.1,Tmax=4.0,points=10,MCSTEPS=15000,SPARE_MCSTEPS=2000):

        """
        Simulation over a temperature range. This function computes:
        - Magnetisation
        - Internal Energy
        - Specific heat
        - Mag. Susceptibility
        """

        # Create array of temperatures
        Temps = [0.0]*int(points)
        deltaT = (Tmax-Tmin)/(points-1)
        for i in range(points):
            Temps[i] = i*deltaT + Tmin
        # Create array of magnetisations
        Mags = [0.0]*int(points)
        # Create array of sqrd magnetisations
        Suscep = [0.0]*int(points)
        # Create array of energies
        Eints = [0.0]*int(points)
        # Create array of sqrd energies
        SpecHeat = [0.0]*int(points)
        # Perform MCMC Steps
        MC_Mag = np.array([0.0]*(MCSTEPS-SPARE_MCSTEPS))
        MC_Eint = np.array([0.0]*(MCSTEPS-SPARE_MCSTEPS))
        for i in range(0,points):
            beta = 1.0/Temps[i]
            # Perform MCMC Steps
            # Spare MC steps while thermalising
            for j in range(SPARE_MCSTEPS):
                self.LatticeMCStep(beta)
            # Compute observables at every MC step
            for j in range(MCSTEPS-SPARE_MCSTEPS):
                self.LatticeMCStep(beta)
                MC_Eint[j] = self.ConfigEnergy()/self.NumSpins
                MC_Mag[j] = abs(self.ConfigMagnetisation())/self.NumSpins
            Mags[i] = np.mean(MC_Mag)
            Eints[i] = np.mean(MC_Eint)
            SpecHeat[i] = (np.std(MC_Eint)**2)*(beta**2)*self.NumSpins
            Suscep[i] = (np.std(MC_Mag)**2)*beta*self.NumSpins

```

```

    return Temps,Mags,Suscep,Eints,SpecHeat

def SingleTempMCMC(self,T = 0.1,MCSTEPS=15000,SPARE_MCSTEPS=2000):
    """
    Computes Important thermodynamic quantities for a single
    temperature. This function might be used with multiprocessing
    module to determine if it speeds up calculations
    """

    MC_Mag = np.array([0.0]*(MCSTEPS-SPARE_MCSTEPS))
    MC_Eint = np.array([0.0]*(MCSTEPS-SPARE_MCSTEPS))
    beta = 1.0/T
    # Perform MCMC Steps
    # Spare MC steps while thermalising
    for j in range(SPARE_MCSTEPS):
        self.LatticeMCStep(beta)
    # Compute observables at every MC step
    for j in range(MCSTEPS-SPARE_MCSTEPS):
        self.LatticeMCStep(beta)
        MC_Eint[j] = self.ConfigEnergy()/self.NumSpins
        MC_Mag[j] = abs(self.ConfigMagnetisation())/self.NumSpins
    Mags = np.mean(MC_Mag)
    Eints = np.mean(MC_Eint)
    SpecHeat = (np.std(MC_Eint)**2)*(beta**2)*self.NumSpins
    Suscep = (np.std(MC_Mag)**2)*beta*self.NumSpins
    return Mags, Eints, SpecHeat, Suscep

def SingleTempMag(self,T = 0.1,MCSTEPS=15000,SPARE_MCSTEPS=2000):
    """
    Computes magnetisation for a single temperature. This Function
    might be used with multiprocessing module to determine critical
    tempererature from critical point of curve.
    """

    MC_Mag = np.array([0.0]*(MCSTEPS-SPARE_MCSTEPS))
    beta = 1.0/T
    # Perform MCMC Steps
    # Spare MC steps while thermalising
    for j in range(SPARE_MCSTEPS):
        self.LatticeMCStep(beta)
    # Compute observables at every MC step
    for j in range(MCSTEPS-SPARE_MCSTEPS):
        self.LatticeMCStep(beta)
        MC_Mag[j] = abs(self.ConfigMagnetisation())/self.NumSpins

```

```

    return np.mean(MC_Mag)

def MagsProfile(\n
    self,Tmin=0.1,Tmax=4.0,points=10,MCSTEPS=15000,SPARE_MCSTEPS=5000):\n
    '''\n
        Simulation over a temperature range. This function computes:\n
        - Magnetisation\n
    '''\n
\n
    # Create array of temperatures\n
    Temps = np.array([0.0]*int(points))\n
    deltaT = (Tmax-Tmin)/(points-1)\n
    for i in range(points):\n
        Temps[i] = i*deltaT + Tmin\n
    # Create array of magnetisations\n
    Mags = np.array([0.0]*int(points))\n
    MC_Mag = np.array([0.0]*(MCSTEPS-SPARE_MCSTEPS))\n
    for i in range(0,points):\n
        beta = 1.0/Temps[i]\n
        # Perform MCMC Steps\n
        # Spare MC steps while thermalising\n
        for j in range(SPARE_MCSTEPS):\n
            self.LatticeMCStep(beta)\n
        # Compute observables at every MC step\n
        for j in range(MCSTEPS-SPARE_MCSTEPS):\n
            self.LatticeMCStep(beta)\n
            MC_Mag[j] = abs(self.ConfigMagnetisation())/self.NumSpins\n
        Mags[i] = np.mean(MC_Mag)\n
    # Compute best fit to MagsFit\n
    fitparams, covmat = curve_fit(\n
        MagsFit,Temps,Mags,bounds=(0,[50.0,50.0,1,0.5,10.0]))\n
    return Temps,Mags,fitparams\n
\n
def Lattice2img(self):\n
    img = np.array(127*np.array(self.Lattice)+128, dtype=np.uint8)\n
    return np.transpose(np.reshape(img, (-1,self.LatticeSize)))\n
\n
def ShowLattice(self):\n
    img = np.array(127*np.array(self.Lattice)+128, dtype=np.uint8)\n
    img = np.reshape(img, (-1,self.LatticeSize))\n
    plt.title(r"Spin Configuration")\n
    plt.imshow(img,cmap='gray')\n
    plt.show()\n
\n
def ThermalAnime(self, T = 0.1, MCSTEPS = 15000, Filename = 'Demo', \

```

```

    save = False):
    fig = plt.figure()
    ims = [None]*(MCSTEPS//300)
    beta = 1.0/T
    for i in range(MCSTEPS):
        self.LatticeMCStep(beta)
        if i%300 == 0:
            im = plt.imshow(self.Lattice2img(), cmap = 'gray', \
            animated = True)
            ims[i//300] = [im]
    ani = animation.ArtistAnimation(fig, ims, interval=1, blit=True, \
repeat_delay=100)
    plt.title(r'Thermalisation of System'+'\n'+r'$T = $ '+str(T))
    plt.show()
    if save:
        ani.save(Filename+'.gif', writer='imagemagick')
        plt.close()

def SimulationTest(self, T = 0.1, MCSTEPS=15000):
    """
    Function for performing thermalisation analysis
    """

    beta = 1.0/T
    MCEints = [0.0]*MCSTEPS
    MCMags = [0.0]*MCSTEPS
    start_time = time.time()
    for i in range(MCSTEPS):
        self.LatticeMCStep(beta)
        MCMags[i] = abs(self.ConfigMagnetisation())/\ \
                    self.NumSpins
        MCEints[i] = self.ConfigEnergy()/\ \
                    self.NumSpins
    end_time = time.time()
    print('Ellapsed Time: ',end_time-start_time)
    # Plot thermalisation
    results, params = plt.subplots(2,1, constrained_layout = True)
    # Plot magnetisation results
    params[0].plot(range(MCSTEPS),MCMags,'ko')
    params[0].set_xlabel('Time (MCs)')
    params[0].set_ylabel('Magnetisation')
    # Plot Energy results
    params[1].plot(range(MCSTEPS),MCEints,'bo')
    params[1].set_xlabel('Time (MCs)')
    params[1].set_ylabel('Energy')

```

```

    results.suptitle('Thermalisation of System \n' + '$T = $ ' + str(T))
    plt.show()

```

#### 14.2.2 Codes for Data generation

Based upon the routines introduced on the previous section, I used the following python program to produce data for all lattice sizes and external fields discussed on section 11.4. This file can be found as **IsingSolver.py** in the project Github repository.

**Important:** To explore the effects of lattice size on the results, change parameter *si* on line 145

```
GenData(mu,hs,si=11)
```

Make sure to run shell script **InitServer.sh** so that Twilio client and the latest Conda distribution are installed on your PC. For this, create a Twilio account and provide your SID and authorisation token. Also, provide a phone number capable of receiving Whatsapp messages that is registered in Colombia. **This script only works on Unix systems.**

```

# Imports for clarity
import numpy as np
import random as rd
import matplotlib.pyplot as plt
import matplotlib.animation as animation
import time
from scipy.optimize import curve_fit
import pandas as pd
# Import twilio client for messaging
from twilio.rest import Client
import os
# Import of the module I wrote for MCMC Simulation
import IsingModel as Alloy
# Set matplotlib style for plotting
# plt.style.use('FigureStyle/PaperStyle.mplstyle')

client = Client()
myphone = os.environ['MYPHONE']

def SaveMagsProfile(\n    s = 8, miu = -10.0, hi = 0.0, points = 30, filename = 'DemoFile',\n    to_num = '1234568090'):

    '''
    Function for data generation and stage control reporting
    using Twilio API
    '''

# Define lattice object

```

```

MyAlloy = Alloy.IsingLattice2D(LatticeSize = s, mu = miu, h = hi)
# Initialise Lattice
MyAlloy.FillNeighbours()
# Initialise Server notification params
server_num = 'whatsapp:+14155238886'
mynum = 'whatsapp:+57'+to_num
# Send starting message
init_message = 'Started Profile Cooking...\n' +\
    'mu = ' + str(miu) + '\n' +\
    'h = ' + str(hi)
client.messages.create(body=init_message,
    from_ = server_num,
    to = mynum)
# Compute Magnetisation profile and best interpolation
start_time = time.time()
Temps, Mags, fitparams = \
MyAlloy.MagsProfile(Tmin=0.05,Tmax=3.5,points=points)
end_time = time.time()
# Send finish cooking message
dt = end_time - start_time
init_message = 'Finished Profile Cooking...\n' +\
    'Elapsed time = ' + str(dt) + '\n' +\
    'Begin saving data to .csv file...'
client.messages.create(body=init_message,
    from_ = server_num,
    to = mynum)
# Convert np.arrays to dataframe
dataset = {
    'Temps':Temps,
    'Mags':Mags,
}
data = pd.DataFrame.from_dict(dataset)
filepath = filename+'.csv'
data.to_csv(filepath,index=False,header=True)
# Send finish writting message
dt = end_time - start_time
init_message = 'Finished saving data...\n' +\
    'A = ' + str(fitparams[0]) + '\n' +\
    'B = ' + str(fitparams[1]) + '\n' +\
    'C = ' + str(fitparams[2]) + '\n' +\
    'D = ' + str(fitparams[3]) + '\n' +\
    'Hope You Have an excellent day ;).'
client.messages.create(body=init_message,
    from_ = server_num,
    to = mynum)
return fitparams

```

```

def GenData(mus, hs, si=4):

    """
    Function for generating and saving all magnetisation data
    and fitting parameters for critical temperature determination
    """

    # Create dictionary to save fitting parameters
    fits = {}
    for i in range(len(mus)):
        for j in range(len(hs)):
            myk = str(i) + '_' + str(j)
            aux = {myk: []}
            fits.update(aux)

    # Start generating and saving data
    for i in range(len(mus)):
        for j in range(len(hs)):
            myk = str(i) + '_' + str(j)
            fname = 'Alt0_Mags_' + myk
            # Compute magnetisation profile, save and returns
            # interpolation data
            fitdata = SaveMagsProfile(\n
                s=si, miu=mus[i], hi=hs[j], points=70, filename=fname,\n
                to_num=myphone)
            # Save interpolation data to file for reference later
            fits[myk] = fitdata

    # Create dataframe for saving fit parameters
    fitsframe = pd.DataFrame.from_dict(fits)
    fitsframe.to_csv('FitParamsT.csv', index=False, header=True)
    # Send finishing message
    server_num = 'whatsapp:+14155238886'
    init_message = 'Finished Cooking Batch...\\n' +\
        'Start pushing results'
    client.messages.create(body=init_message,
                           from_=server_num,
                           to='whatsapp:+57' + myphone)

def PlotMagsProfile(filepath, fitparams, use_fit = True):
    # Read generated data into DataFrame
    dataset = pd.read_csv(filepath)
    # Generate Fit curve
    if use_fit:

```

```

x = np.linspace(0.05,2.5,num=300)
y = Alloy.MagsFit(x,*fitparams)
# Plot dataset
plt.scatter(dataset['Temps'],dataset['Mags'])
if use_fit:
    plt.plot(x,y)
plt.xlabel(r'$k_BT/Jz$')
plt.ylabel(r'$\langle M \rangle$')
plt.show()

if __name__ == '__main__':
    #fitparams = SaveMagsProfile(
    #s=8,miu=-10.0,hi=0.0,points=26,filename='TestFile',to_num='3158009152')

    #fitparams = []
    #PlotMagsProfile('Mags_1_1.csv',fitparams,use_fit=False)
    # mu1 = [0.0,-0.7]
    # mu = [0.0,-1.7]
    # hs = [0.0,0.1,0.3,0.5]

    mu = [0.0,-1.7]
    hs = [0.0,0.1,0.3,0.5]
    GenData(mu,hs,si=11)

```

To visualize alloy configuration, use python script **IsingGrapher.py**. Provide as arguments the index of  $\mu$  and  $h$  according to the Google Colab notebook key (presented in the next section), and also an extra argument stating whether to save the animation or not.

**Important:** In case of any doubt, do not hesitate writing to *diegohererra262@gmail.com* to discuss this codes and the results of this project

### 14.3 Google Colab Notebook For Data Processing

This notebook contains two main components:

- Mean Field Numerical Calculations
- Data Processing from MCMC simulations

The source code is available at the project's repository. It is suggested that the notebook be run from the first cell to the last cell in order. This would recreate the tasks carried out to fulfill the project's objectives in chronological and methodological order.

**Important:** This notebook is designed for Unix users only. If the only OS available is Microsoft Windows, change filepaths accordingly.

# ProjectDataProcessing

November 29, 2020

## 1 Mean Filed Approximation for BEG Model for a Nonstoichiometric Binary Alloy with Vacancies

I will consider the analytical calculations concerning **mean field approximation** for a simple ferromagnetic Blume - Capel model with a staggered external magnetic field, in a bipartite lattice with coordination number  $z$ :

$$H = -\frac{J}{2} \sum_{\langle i_A, i_B \rangle} S_i S_j + \frac{K}{2} \sum_{\langle i_A, i_B \rangle} S_i^2 S_j^2 + \mu \sum_i S_i^2 + h \sum_{i_A} S_i - h \sum_{i_B} S_i$$

Where  $A$  and  $B$  are the two neighbouring sublattices on the general lattice structure, containing  $N$  sites.

**Important:** The limit  $\mu \rightarrow -\infty$  corresponds to zero vacancy concentration. The limit  $h = 0$  corresponds to a stoichiometric lattice. Both limits are equivalent to a simple Ferromagnetic Ising Model.

### 1.1 GBF Variational Method for Mean Field Approximations

The procedure is fairly straightforward. I used variational Hamiltonian:

$$\hat{H} = -\gamma_A \sum_{i_A}^{N/2} S_i + \alpha_A \sum_{i_A}^{N/2} S_i^2 - \gamma_B \sum_{i_B}^{N/2} S_i + \alpha_B \sum_{i_B}^{N/2} S_i^2$$

Computed variational estimation of free energy at inverse temperature  $\beta$ :

$$\frac{\hat{F}}{N} = \langle S_{i_A} \rangle \left[ \frac{\gamma_A}{2} - \frac{Jz}{4} \langle S_{i_B} \rangle - \frac{h}{2} \right] + \langle S_{i_B} \rangle \left[ \frac{\gamma_B}{2} - \frac{Jz}{4} \langle S_{i_A} \rangle + \frac{h}{2} \right] + \langle S_{i_A}^2 \rangle \left[ -\frac{\alpha_A}{2} + \frac{Kz}{4} \langle S_{i_B}^2 \rangle + \frac{\mu}{2} \right] + \langle S_{i_B}^2 \rangle \left[ -\frac{\alpha_B}{2} + \frac{Kz}{4} \langle S_{i_A}^2 \rangle \right]$$

Where the sublattice one-site partition functions are defined

$$Z_A = 1 + 2e^{-\beta\alpha_A} \cosh(\beta\gamma_A)$$
$$Z_B = 1 + 2e^{-\beta\alpha_B} \cosh(\beta\gamma_B)$$

And expected values can be computed as follows

$$\begin{aligned}\langle S_{i_A} \rangle &= \frac{2}{N} \sum_{i_A} S_i = \frac{1}{\beta} \frac{\partial}{\partial \gamma_A} \ln(Z_A) \\ \langle S_{i_B} \rangle &= \frac{2}{N} \sum_{i_B} S_i = \frac{1}{\beta} \frac{\partial}{\partial \gamma_B} \ln(Z_B) \\ \langle S_{i_A}^2 \rangle &= \frac{2}{N} \sum_{i_A} S_i^2 = -\frac{1}{\beta} \frac{\partial}{\partial \alpha_A} \ln(Z_A) \\ \langle S_{i_B}^2 \rangle &= \frac{2}{N} \sum_{i_B} S_i^2 = -\frac{1}{\beta} \frac{\partial}{\partial \alpha_B} \ln(Z_B)\end{aligned}$$

Minimization of variational free energy with respect to variational parameters lead to:

$$\begin{aligned}\gamma_A &= Jz \langle S_{i_B} \rangle + h \\ \gamma_B &= Jz \langle S_{i_A} \rangle - h \\ \alpha_A &= Kz \langle S_{i_B}^2 \rangle + \mu \\ \alpha_B &= Kz \langle S_{i_A}^2 \rangle + \mu\end{aligned}$$

Defining variables

$$\begin{aligned}m_A &= \langle S_{i_A} \rangle \\ m_B &= \langle S_{i_B} \rangle \\ q_A &= \langle S_{i_A}^2 \rangle \\ q_B &= \langle S_{i_B}^2 \rangle\end{aligned}$$

Which are related to the order parameter of the transition  $m = m_A + m_B$ , and vacancy concentration  $1 - x = q_A + q_B$ , the following consistency equations are derived

$$\begin{aligned}m_A &= \frac{2 \sinh(\beta[Jzm_B + h])}{e^{\beta(Kzq_B + \mu)} + \cosh(\beta[Jzm_B + h])} \\ q_A &= \frac{2 \cosh(\beta[Jzm_B + h])}{e^{\beta(Kzq_B + \mu)} + \cosh(\beta[Jzm_B + h])} \\ m_B &= \frac{2 \sinh(\beta[Jzm_A - h])}{e^{\beta(Kzq_A + \mu)} + \cosh(\beta[Jzm_A - h])} \\ q_B &= \frac{2 \cosh(\beta[Jzm_A - h])}{e^{\beta(Kzq_A + \mu)} + \cosh(\beta[Jzm_A - h])}\end{aligned}$$

If the vacancy - atom bond interplay is such that  $K = 0$ , the above stated equations simplify dramatically:

$$m_A = \frac{2 \sinh(\beta[Jzm_B + h])}{e^{\beta\mu} + \cosh(\beta[Jzm_B + h])}$$

$$q_A = \frac{2 \cosh(\beta[Jzm_B + h])}{e^{\beta\mu} + \cosh(\beta[Jzm_B + h])}$$

$$m_B = \frac{2 \sinh(\beta[Jzm_A - h])}{e^{\beta\mu} + \cosh(\beta[Jzm_A - h])}$$

$$q_B = \frac{2 \cosh(\beta[Jzm_A - h])}{e^{\beta\mu} + \cosh(\beta[Jzm_A - h])}$$

## 1.2 Redefinition in Terms of Order Parameter

For a more direct interpretation of the above system, from which only the first two are of practical importance, I change to variables

$$m = \frac{m_A + m_B}{2}$$

$$n = \frac{m_A - m_B}{2}$$

Notice that  $m$  corresponds exactly to the order parameter of the transitions, and  $n$  is directly related to atom concentration. For low vacancy concentration,  $n \approx 2x - 1$ . Now, the consistency equations may be rewritten

$$m + n = f(m - n + h)$$

$$m - n = f(m + n - h)$$

With the definition

$$f(u) = \frac{2 \sinh(\beta u)}{e^{\beta\mu} + 2 \cosh \beta u}$$

Notice a trivial set of solutions

$$m_0 = 0$$

$$n_0 = f(h - n_0)$$

In this notebook I set out to

1. Solving the Above system numerically to establish the nature of phase transitions in the parameter range  $|h| \leq h_0, T \leq 1/3$
2. Generate plots of magnetisation as a function of temperature for several field values (i.e. different equilibrium concentrations) To determine the nature of phase transitions

Continous Phase transitions imply continous magnetization-temperature profile. Discontinuous phase transitions imply discontinous magnetization-temperature profile.

**Important:** Analytical calculations have already been performed by hand.

```
[1]: # Do you have a latex distro on your PC?  
latex_in_my_pc = True
```

```
[127]: # Imports for clarity  
import numpy as np  
import random as rd  
import matplotlib.pyplot as plt  
import matplotlib.animation as animation  
import time  
from scipy.optimize import fsolve  
from scipy.optimize import curve_fit  
from scipy.stats import linregress  
import pandas as pd  
# Import of the module I wrote for MCMC Simulation  
import IsingModel as Alloy  
if latex_in_my_pc:  
    plt.style.use('FigureStyle/PaperStyle.mplstyle')
```

## 1.3 Definition of important parameters

### 1.3.1 Thermodynamic parameters

1.  $\mu$ : Related to vacancy-atom chemical potential difference
2.  $\beta$ : Inverse temperature
3.  $h$ : Related to atom chemical potential difference

```
[46]: # Thermodynamic parameters  
mu = -10.1  
h = 0.0  
  
# Auxiliar functions for numerical solutions  
  
def f(x, beta, miu):  
    ...  
    Function that appears everywhere on calculations  
    ...  
    return 2*np.sinh(beta*x)/(np.exp(beta*miu) + 2*np.cosh(beta*x))  
  
def FixedPoint(x,beta,miu):  
    ...  
    Function for computing equilibrium atom concentration  
    ...
```

```

    return x - f(h/4-x,beta, miu)

def ConsFunc(ms,beta, miu):
    """
    Function for numerically solving consistency equations
    """
    return [f((ms[0] - ms[1] + h),beta,miu) - (ms[0] + ms[1]), \
            f((ms[0] + ms[1] - h),beta,miu) - (ms[0] - ms[1])]

def n0(beta,miu):
    """
    Auxiliar functions for numerical solutions
    """
    def fn(x):
        return FixedPoint(x,beta,miu)

    s = fsolve(fn,[0.5])
    return s[0]

def ConsFuncSol(beta,miu):
    """
    Numerical solution of consistency equations
    """
    def func(ms):
        return ConsFunc(ms,beta,miu)

    init = [0.7, 0.2]
    if h < 0:
        init = [-0.7, -0.2]
    sols = fsolve(func,init)

    return sols[0], sols[1]

```

```
[48]: Ts = np.linspace(0.01,1.5,num = 8000)

ms = {1: [],  
      2: [],  
      3: []}  
  
ns = {1 : [],  
      3 : [],  
      2 : []}  
  
mus = [0.0, -0.7, -10.0]  
  
counter = 1  
for mu in mus:
```

```

for T in Ts:
    m, n = ConsFuncSol(1.0/T,mu)
    ms[counter].append(abs(m))
    ns[counter].append(abs(n))
    counter += 1

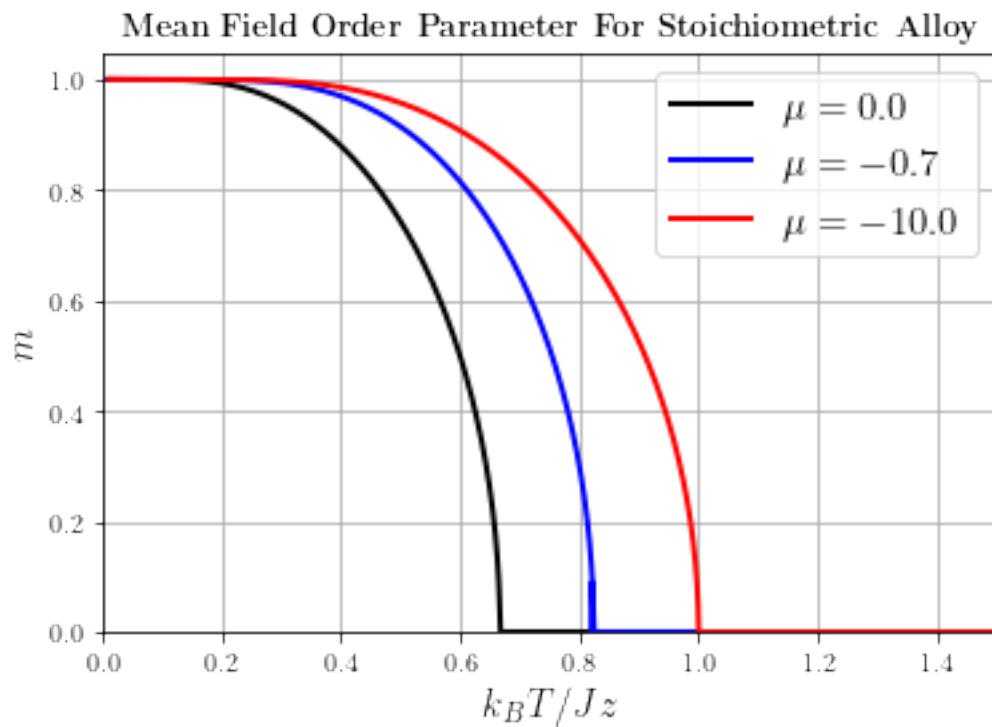
```

```
[49]: # Save plot
save_ = True
```

```

[50]: plt.plot(Ts,ms[1],linewidth = 2.0,color = 'k',label = r'$\mu = 0.0$')
plt.plot(Ts,ms[2],linewidth = 2.0,color = 'b',label = r'$\mu = -0.7$')
plt.plot(Ts,ms[3],linewidth = 2.0,color = 'r',label = r'$\mu = -10.0$')
plt.xlim([0.0,1.5])
plt.ylim([0.0,1.05])
plt.title(r'\textbf{Mean Field Order Parameter For Stoichiometric Alloy}')
plt.xlabel(r'$k_B T / Jz$',fontsize = 15)
plt.ylabel(r'$m$',fontsize = 15)
plt.legend(fontsize = 15)
if save_:
    plt.savefig('Figures/MeanFieldMags.pdf')
    plt.savefig('Figures/MeanFieldMags.png')
plt.show()

```



## 1.4 Computation of Critical Curve in $h - T$ Plane

By considering the system of consistency equations near  $m = 0, n = n_0$ , I derived the following implicit equation for the critical curve

$$f'(h - n)|_{n=n_0} = 1$$

Solving this equation analytically is not convenient since  $f$  is not a particularly simple function. However, I will solve it numerically for fixed  $\mu$ . It must be that in the limit  $\mu \rightarrow -\infty$ , the results from Porta and Castán are recovered.

By now, I shall consider some limit cases of the curve. If  $h = 0$ , the results reduce to that of Blume, Emery and Griffiths. Critical temperature depends on chemical potential  $\mu$ , and if

$$\mu \rightarrow -\infty, T_c \rightarrow 1$$

On the other hand, if  $T_c \rightarrow 0$ , the system tends to the all-parallel spin state. The minimum energy is

$$E_{min} = -N/2 + \mu N$$

On the other hand, If the field is intense enough, the energy might be lowered if the system transits to an staggered spin configuration, i.e. all spins antiparallel. The boundary of this transition is such that

$$h_c(T_c = 0) = 1$$

**Important:** Unit energy is  $Jz$  and unit entropy is  $k_B$ .

```
[43]: mu = 0.00

def f(x, beta, field, miu):
    """
    Function that appears everywhere on calculations
    """
    return 2*np.sinh(beta*(field-x))/(np.exp(beta*miu) + 2*np.
    →cosh(beta*(field-x)))

def fp(x, beta, field, miu):
    """
    Derivative that appears on critical curve
    """
    return beta * (2*np.cosh(beta*(field-x))/
        (np.exp(beta*miu) + 2*np.cosh(beta*(field-x))) - f(x, beta,
    →field, miu)**2)

def FixedPoint(x,beta,field,miu):
```

```

    ...
Function for computing equilibrium atom concentration
    ...

return x - f(x,beta,field,miu)

def Func(beta, field, miu):
    def root(x):
        return FixedPoint(x,beta,field,miu)
    s = fsolve(root,[0.1])
    return s[0]

def CritField(beta,miu):
    def CostFunc(field):
        n = Func(beta, field, miu)
        return fp(n,beta,field,miu) - 1
    seed = [1 - 1.0/beta]
    if beta >= 1:
        seed = [0.01]
    fld = fsolve(CostFunc,seed)
    return fld[0]

def ZeroFieldBeta(miu):
    def Cf(beta):
        return beta/(1 + 0.5*np.exp(beta*miu)) - 1
    seed = [0.5]
    b = fsolve(Cf,seed)
    return b[0]

```

```

[44]: hs = {1: [],
           2: [],
           3: []}

mus = [0.0, -0.7, -10.0]

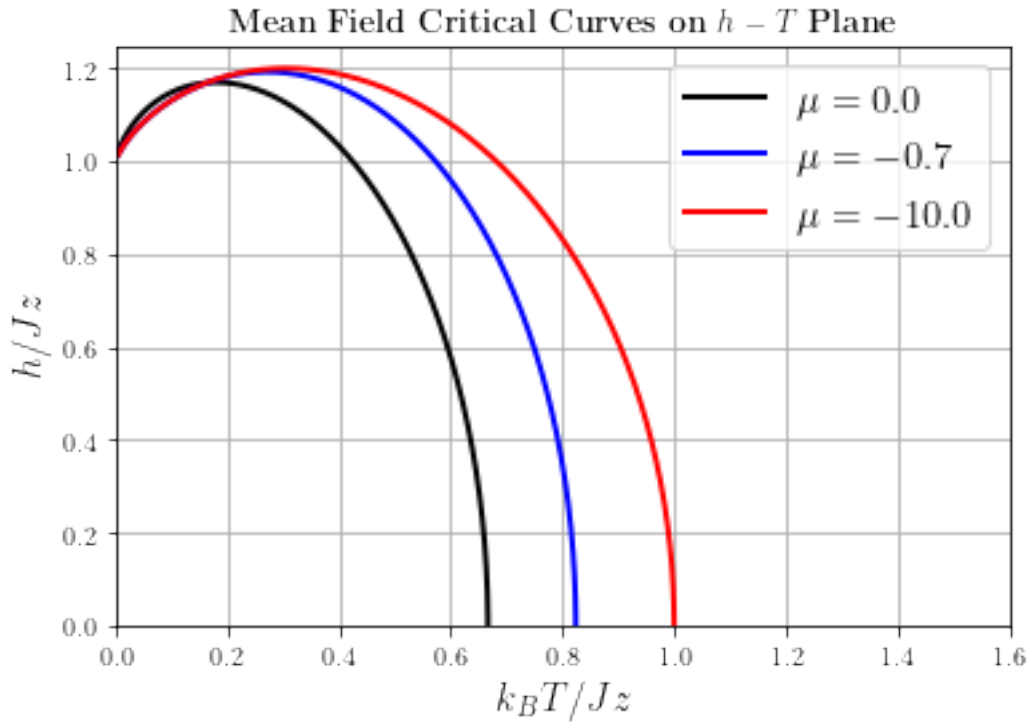
Ts = {
    1 : np.linspace(0.005,1.0/ZeroFieldBeta(mus[0]),num = 8000),
    2 : np.linspace(0.005,1.0/ZeroFieldBeta(mus[1]),num = 8000),
    3 : np.linspace(0.005,1.0/ZeroFieldBeta(mus[2]),num = 8000)
    }

counter = 1
for miu in mus:
    for T in Ts[counter]:
        h = CritField(1.0/T,miu)
        hs[counter].append(abs(h))
    counter += 1

```

```
[41]: # Save figure
save_ = True

[45]: plt.plot(Ts[1],hs[1],linewidth = 2.0,color = 'k',label = r'$\mu = 0.0$')
plt.plot(Ts[2],hs[2],linewidth = 2.0,color = 'b',label = r'$\mu = -0.7$')
plt.plot(Ts[3],hs[3],linewidth = 2.0,color = 'r',label = r'$\mu = -10.0$')
plt.xlim([0.0,1.6])
plt.ylim([0.0,1.25])
plt.title(r'\textbf{Mean Field Critical Curves on} $h-T$ \textbf{Plane}')
plt.xlabel(r'$k_B T / Jz$',fontsize = 15)
plt.ylabel(r'$h / Jz$',fontsize = 15)
plt.legend(fontsize = 15)
if save_:
    plt.savefig('Figures/MeanFieldCritCurveshT.pdf')
    plt.savefig('Figures/MeanFieldCritcurveshT.png')
plt.show()
```



## 1.5 Computation of Critical Curve in $x - T$ Plane

Note that the parameter

$$n = \frac{m_A - m_B}{2}$$

Is directly related to concentration difference between A type atoms and B type atoms. Also note that

$$q_A + q_B$$

Is directly related to vacancy concentration. I shall define

$$2x - 1 = \frac{N_A - N_B}{N} = n$$

In the limit of low vacancy concentration,  $x$  is directly related to atom concentration. I need to compute  $n$  on the critical line of order-disorder transitions on plane  $h - T$ , and this would directly lead to a critical curve on  $x - T$  plane.

**Important:** Unit energy is  $Jz$  and unit entropy is  $k_B$ .

```
[18]: def conc(beta,h,miu):
    return (Func(beta,h,miu) + 1)*0.5
```

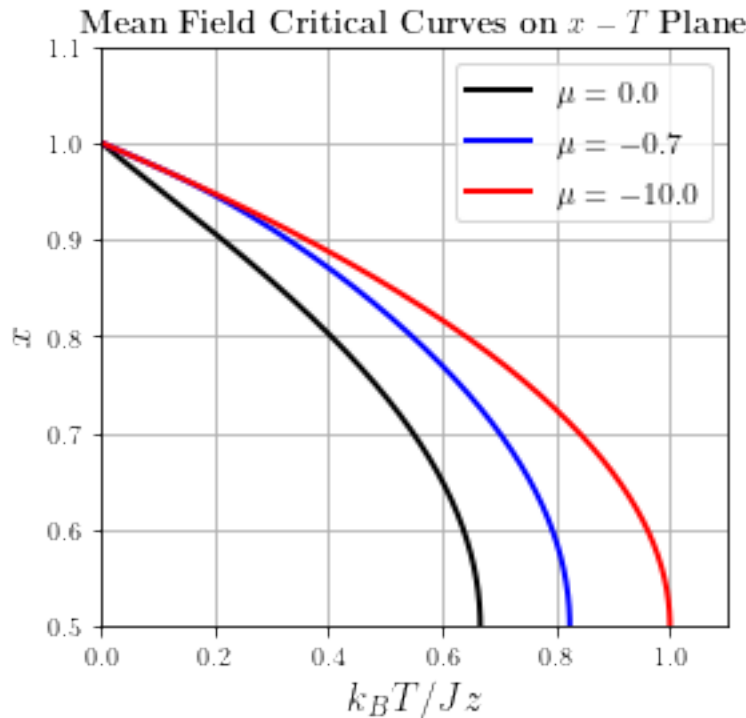
```
[19]: xs = {1: [], 2: [], 3: []}

counter = 1
for miu in mus:
    for T,h in zip(Ts[counter], hs[counter]):
        c = conc(1.0/T, h, miu)
        xs[counter].append(abs(c))
    counter += 1
```

```
[24]: # Save figure
save_ = True
```

```
[25]: fig = plt.figure()
ax = fig.add_subplot(111)
plt.xlim([0.0,1.1])
plt.ylim([0.5,1.1])
ax.plot(Ts[1],xs[1],linewidth = 2.0,color = 'k',label = r'$\mu = 0.0$')
ax.plot(Ts[2],xs[2],linewidth = 2.0,color = 'b',label = r'$\mu = -0.7$')
ax.plot(Ts[3],xs[3],linewidth = 2.0,color = 'r',label = r'$\mu = -10.0$')
ax.set_aspect(aspect = 1.7)
plt.title(r'\textbf{Mean Field Critical Curves on} $x-T$ \textbf{Plane}')
plt.xlabel(r'$k_B T / Jz$', fontsize = 15)
plt.ylabel(r'$x$', fontsize = 15)
plt.legend(fontsize = 12)
if save_:
    plt.savefig('Figures/MeanFieldCritCurvesxT.pdf')
    plt.savefig('Figures/MeanFieldCritcurvesxT.png')
```

```
plt.show()
```



## 2 Data Processing Of MCMC Simulation Data from Binary Alloy

The main objective of this notebook is to document and illustrate all data analysis for determination of critical temperatures and graphics generation for my Theoretical Investigations Project. I have already determined mean field critical curves for the BEG model, and in this notebook I set out to:

1. Produce Order Parameter profiles for several values of vacancy and atom chemical potential difference.
2. Compute critical temperatures for several Lattice sizes and vacancy - atom chemical potential difference.
3. Use finite size scaling to determine a set of critical points in  $h - T$  phase space projection.

**Note:** During the development of this phase of the project, I updated my PC to MacOs Big Sur. This had the unexpected effect of slowing python scripts. As a result, I resorted to using an Azure server with 2 vcpus and 8GB of RAM. Most of the data used in this project was generated on that server. It took about 2 weeks of computation to generate order parameter data for all lattice sizes. I had parallelised routines to fasten computation of magnetisation profiles, they were pointless on my Azure server since it has only 2 vcpus.

## 2.1 Order Parameter Profiles for Different Lattice Sizes and Chemical Potential Differences

Remember that the sampled Hamiltonian corresponds to a ferromagnetic BEG Model, on a centered rectangular lattice, with a non-zero quadrupolar anisotropy term, in the presence of an staggered external magnetic field:

$$H = -\frac{J}{2} \sum_{\langle i_{A_2}, j_{B_2} \rangle} S_{i_{A_2}} S_{j_{B_2}} + \mu \sum_i S_i^2 + h \sum_{i_B} S_{i_B} - h \sum_{i_A} S_{i_A}$$

I used conventional MCMC (Markov Chain Monte Carlo) to sample the Gibbs-Boltzmann distribution corresponding to this system. Just to remember, the system under study is a bipartite, substitutional, non-stoichiometric, binary alloy. I used MCMC techniques to compute equilibrium values of order parameter:

$$m = \langle S_{i_{A_2}} \rangle + \langle S_{i_{B_2}} \rangle$$

I know that order parameter profile depends not only on temperature, but also on lattice size. Therefore, I computed several datasets corresponding to different values of  $\mu$ ,  $h$ , temperature ( $T$ ) and lattice size ( $L$ ). I normalised unit energies so that  $J = 1$ , and units of entropy so that Boltzman's constant,  $k_B = 1$ .

Each dataset corresponds to magnetisation for 30 equally spaced temperatures between  $T_{\min} = 0.05$  and  $T_{\max} = 3.5$ . I computed magnetisation profiles for values  $\mu = 0.0, -1.7$  and  $h = 0.0, 0.1, 0.3, 0.5$ . Datasets corresponds to lattice sizes  $L = 8, 16, 32, 55$ . The dataset files are saved as csv, and the names are `AltL_Mags_mu_h.csv`, in accordance to the following convention:

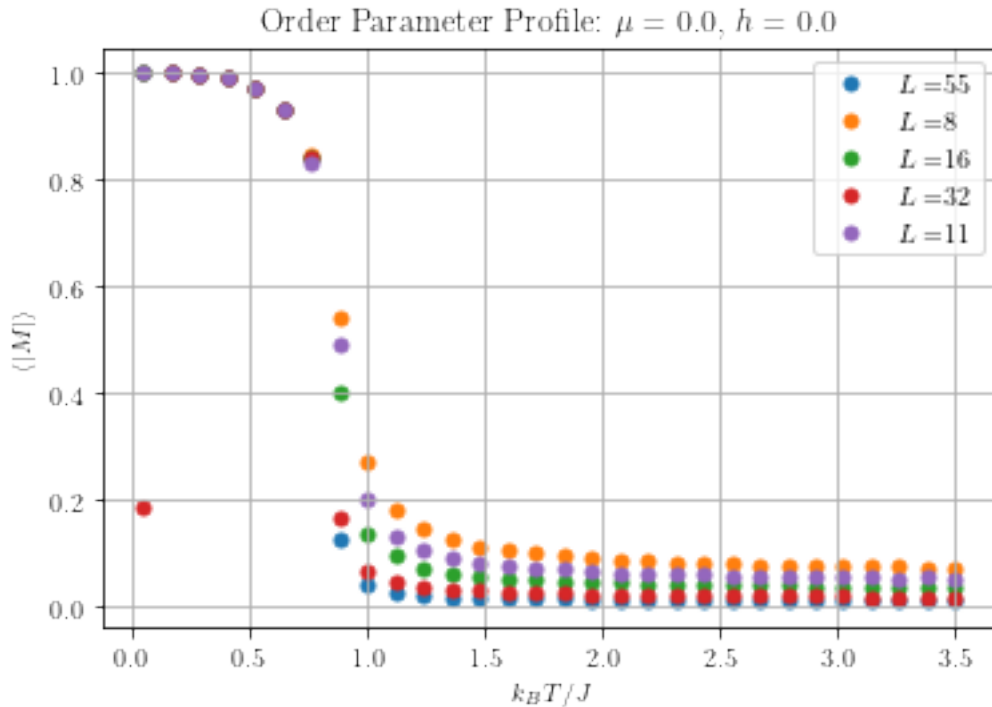
Index	$L$	$\mu$	$h$
0	55	0	0.0
1	8	-1.7	0.1
2	16	-	0.3
3	32	-	0.5
4	11	-	-

**Important:** MCMC Simulations consisted on 15000 steps, with 5000 spare steps.

```
[54]: # Define keys for plotting
Lkey = [55,8,16,32,11]
Mukey = [0.0,-1.7]
hkey = [0.0,0.1,0.3,0.5]
```

```
[119]: # Read all data files corresponding to indexes following table above and store
        ↪data for plotting
Muidx = '0'
hidx = '0'
save_ = False
```

```
[122]: for i in range(5):
    # Reading with pandas
    filepath = 'Data/Alt'+str(i) +'_'+ 'Mags_ '+Muidx+'_'+hidx+'.csv'
    dataset = pd.read_csv(filepath)
    # Generate scatter plot
    plt.scatter(dataset['Temps'],dataset['Mags'],label=r'$L=$'+str(Lkey[i]))
plt.xlabel(r'$k_BT/J$')
plt.ylabel(r'$\langle M \rangle$')
plt.title(r'Order Parameter Profile: '+r'$\mu=$' +str(Mukey[int(Muidx)])+r', ' +
    r'$h=' +str(hkey[int(hidx)])) )
plt.legend()
if save_:
    plt.savefig('Figures/+'+MagsProf_+Muidx+'_'+hidx+'.pdf')
    plt.savefig('Figures/+'+MagsProf_+Muidx+'_'+hidx+'.png')
plt.show()
```



In the above cell, a quick overview of the datasets simulated via MCMC can be obtained. A quite unexpected magnetisation profile was obtained when  $h > 0$ . Although the curve seems to have a critical point, lattice size does not seem to affect the equilibrium magnetisation. This is rather weird, since at a critical point, correlation length diverges, and the finiteness of the system should affect the magnetisation profile. As is evident from the Hamiltonian, the value of  $\mu$ , which is related to vacancy concentration, is not responsible for this behavior. The presence of a non-zero staggered field causes a non-zero order parameter even at high temperatures. This is readily seen from a magnetic interpretation of the interaction Hamiltonian. Also, remembering that the

order parameter is also related to atom concentration difference, this can be intuited.

**Conjecture:** It might be possible that for high staggered field magnitude, this phenomenon competes strongly with the inherent lattice site correlation, thus diminishing significantly the dependence of the order parameter profile with lattice size.

## 2.2 Computation of critical temperatures

I compute critical temperatures by interpolating order parameter data, and computing the inflection point. Although my simulations showed rather strange profiles for non stoichiometric alloys, there still present an inflection point, which I will use to estimate critical temperature. I will, however, use finite size scaling to determine the actual critical temperature of a stoichiometric binary alloy for the values of  $\mu$  considered.

### 2.2.1 Data Interpolation

I chose the function

$$f(x) = A \tanh(C - Dx) + B$$

To interpolate the order parameter data. Although this function might not be the best for this purpose, it allows easy estimation of critical temperature as

$$T_C(L) = \frac{C}{D}$$

In the next cell, I plot inverse critical temperature as function of inverse lattice size following Ibarra and others' work.

**Important:** Spin-1 Ising Models do not have a closed form for order parameter as function of temperature, like Onsager's solution to the Spin-1/2 Ising model on 2 dimensions. Ibarra proposes a fit of the type

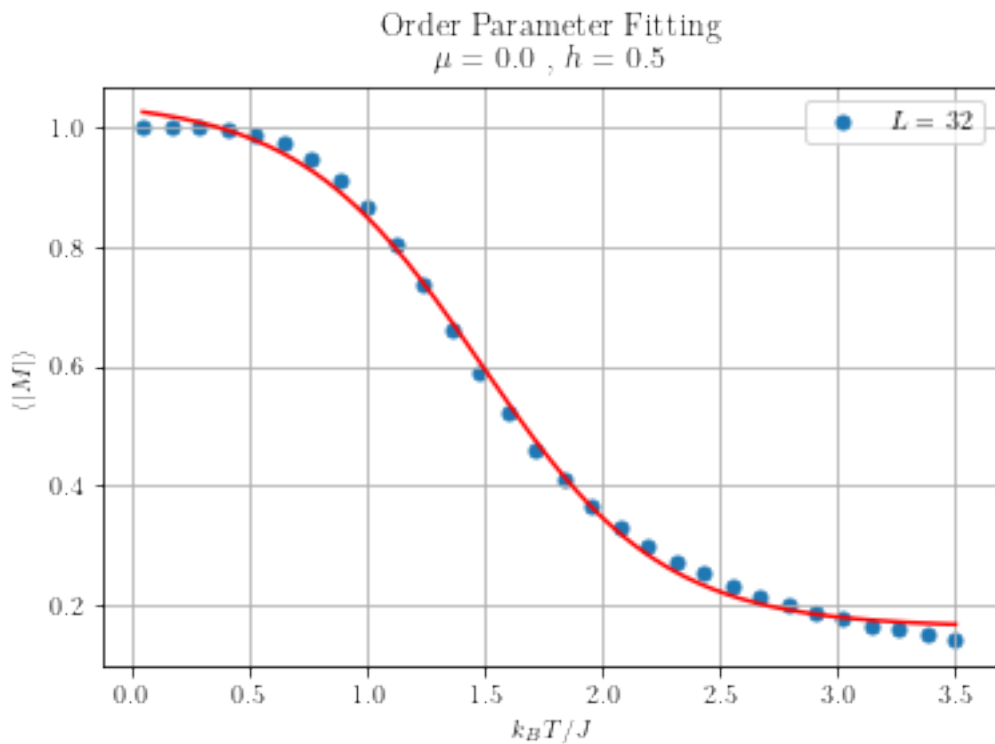
$$m = \left[ A - B \left( \sinh \left( \frac{2}{T} \right) \right)^{-4} \right]^C$$

But this is valid only for temperatures below  $T_C$ , which I want to find. Therefore, it is not a very good option for fitting the data.

```
[57]: # Interpolation Function
def magsFit(x,A,B,C,D):
    return A*np.tanh(C-D*x)+B
```

```
[58]: # Indexes for reading data
Muidx = '0'
hidx = '3'
Lidx = '3'
# Tag to tell program if saving plots
save_ = False
```

```
[59]: # Reading with pandas
filepath = 'Data/Alt'+Lidx+'_'+Mags_+Muidx+'_'+hidx+'.csv'
dataset = pd.read_csv(filepath)
# Interpolate using scipy
fitparams, covmat = curve_fit(
    magsFit,dataset['Temps'],dataset['Mags'],\
    bounds=(0,[50.0,50.0,50.0,50.0]))
# Plot Interpolation and dataset
x = np.linspace(0.05,3.5,num=300)
y = magsFit(x,*fitparams)
plt.scatter(dataset['Temps'],dataset['Mags'],label=r'$L=$ '+str(Lkey[int(Lidx)]))
plt.plot(x,y,color='r')
plt.xlabel(r'$k_BT/J$')
plt.ylabel(r'$\langle M \rangle$')
plt.title(\n    r'Order Parameter Fitting'+\n    r'$\mu = $ '+str(Mukey[int(Muidx)])+\n    r'$h = $ '+str(hkey[int(hidx)]))
plt.legend()
if save_:
    plt.savefig('Figures/''Fit'+Lidx+'_'+Muidx+'_'+hidx+'.pdf')
    plt.savefig('Figures/''Fit'+Lidx+'_'+Muidx+'_'+hidx+'.png')
plt.show()
```



## 2.2.2 Finite Size Scaling

Although the non linear fit is not the best, specially for stoichiometric alloys, I believe this is the best way I can find to compromise MCMC simulation time and precision in critical temperature computation. More in depth calculations should require use of reweighting techniques, and several dataset evaluations in order to compute mean order parameter profiles with appropriate error bars. However, due to time constraints, and a miscalculation of the time required for the analytical component of this project, I use this procedure to estimate critical temperature for an infinite lattice.

```
[90]: # Fix fields values
Muidx = '1'
hidx = '1'
# Tag to tell program if saving plots
save_ = False

[93]: Tcs = [0,0,0,0,0]
# Reading with pandas
for Lidx in range(5):
    filepath = 'Data/Alt'+str(Lidx) + '_'+'Mags_'+Muidx+'_'+hidx+'.csv'
    dataset = pd.read_csv(filepath)
    # Eliminate first point since it was an outsider for L = 32
    m = dataset['Mags'][1:]
    T = dataset['Temps'][1:]
    # Interpolate using scipy
    fitparams, covmat = curve_fit(
        magsFit,T,m,
        bounds=(0,[50.0,50.0,50.0,50.0]))
    # Compute critical temperature
    Tcs[Lidx] = fitparams[2]/fitparams[3]

    # Perform linear fit to find critical temperature
    Bc = 1/np.array(Tcs)
    Linv = 1/np.array(Lkey)
    slope, intercept, _, _, _ = linregress(Linv,Bc)
    Lsint = np.linspace(0.01,0.13,num=200)
    Bcint = slope*Lsint + intercept

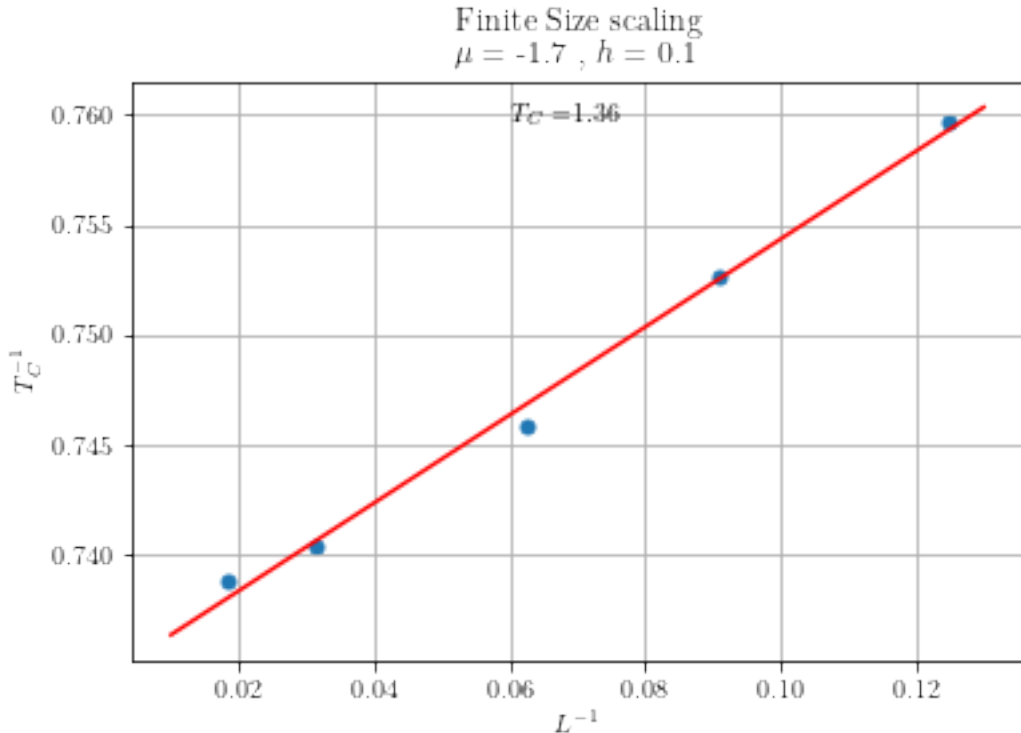
    # Plot Critical Temperatures
    plt.scatter(Linv,Bc)
    plt.plot(Lsint,Bcint,color='r')
    plt.xlabel(r'$L^{-1}$')
    plt.ylabel(r'$T_C^{-1}$')
    plt.text(0.06,np.amax(Bc),r'$T_C = $'+'{:2f}'.format(1/intercept))
    plt.title(r'Finite Size scaling'+'\n'+r'$\mu = $ '+str(Mukey[int(Muidx)])+',
              r'$h = $ '+str(hkey[int(hidx)]))

    if save_:
        plt.savefig('Figures/''FiniteSize_'+Muidx+'_'+hidx+'.pdf')
```

```

plt.savefig('Figures/+'+FiniteSize_+Muidx+'_'+hidx+'.png')
plt.show()
print(r'T_c = ',1/intercept)

```



$T_c = 1.3616706078089678$

As can be seen in the cell above, the finite size scaling technique proposed by Ibarra suits quite good the critical temperature dependance on lattice size. The linear fit, however is not particularly good for stoichiometric alloys, but this might be due to the fact that the non linear fit of magnetisation profile is not particularly good for these datasets (*go to Data Interpolation*). I thus proceed to compute a table with all critical temperature data, for different values of external fields.

```
[62]: def Tcrit(muidx,hidx):
    Tcs = [0,0,0,0,0]
    # Reading with pandas
    for Lidx in range(5):
        filepath = 'Data/Alt'+str(Lidx) + '_' +'Mags_'+Muidx+'_'+hidx+'.csv'
        dataset = pd.read_csv(filepath)
        # Eliminate first point since it was an outsider for L = 32
        m = dataset['Mags'][1:]
        T = dataset['Temps'][1:]
        # Interpolate using scipy
        fitparams, covmat = curve_fit(\
```

```

    magsFit,T,m,\n
    bounds=(0,[50.0,50.0,50.0,50.0]))\n
    # Compute critical temperature\n
    Tcs[Lidx] = fitparams[2]/fitparams[3]\n\n
    # Perform linear fit to find critical temperature\n
    Bc = 1/np.array(Tcs)\n
    Linv = 1/np.array(Lkey)\n
    slope, intercept, _, _, _ = linregress(Linv,Bc)\n
    return 1/intercept

```

[63]: Muidx = '0'  
save\_ = False

[64]: Ts = []  
h = []  
# Compute critical temperatures  
for hidx in ['0','1','2','3']:  
 h.append(hkey[int(hidx)])  
 Ts.append(Tcrit(Muidx,hidx))  
# Create dictionary previous to dataframe  
data = {  
 'h':h,  
 'Tcrit':Ts  
}  
# Create dataframe  
data = pd.DataFrame.from\_dict(data)  
if save\_:  
 filepath = 'Data/CritTemps'+Muidx+'.csv'  
 data.to\_csv(filepath,index=False,header=True)  
# Display Critical temperatures  
display(data)

	h	Tcrit
0	0.0	0.808997
1	0.1	1.083204
2	0.3	1.317169
3	0.5	1.495747

## 2.3 Final MCMC Results

After performing linear regressions from finite size scaling, I obtained the following critical temperatures for  $\mu = 0$ :

$$\frac{\overline{h}}{\overline{T_C}} = \frac{0.0}{0.809}$$

$h$	$T_C$
0.1	1.083
0.3	1.317
0.5	1.496

And the following for  $\mu = -1.7$

$h$	$T_C$
0.0	1.044
0.1	1.362
0.3	1.644
0.5	1.844

These are astonishing results that were not expected from mean field calculations.

## 2.4 Demonstration of Thermal Equilibration using MCMC

I show here an animation of the thermal equilibration of the alloy to illustrate the vacancy assisted dynamics of the ordering process.

**Note:** The image shows the two sublattices of the alloy. The left corresponds to  $A_2$ , and the right, to  $B_2$ .

```
[85]: ! python IsingGrapher.py 0 3 2.809 True
! open Animations/*
```

Figure (640x480)

## 2.5 Computation of Important Thermodynamical Quantities

I am confident enough to assert that increasing vacancy concentration decreases critical temperature, as mean field calculations and MCMC simulations confirm. I also computed critical temperatures for a stoichiometric alloy, which are consistent with the tendency reported by Ibarra. However, to characterise better the critical behavior of non stoichiometric alloys, I compute other thermodynamical quantities:

- Internal Energy
- Specific Heat
- Derivative of Order Parameter

```
[128]: Muidx = '0'
hidx = '3'
save_ = False
```

```
[129]: # Create Alloy Object for simulation
myAlloy = Alloy.IsingLattice2D\
(LatticeSize=16, mu=Mukey[int(Muidx)], h=hkey[int(hidx)])
```

```

# Initialise Lattice
myAlloy.FillNeighbours()
# Compute thermodynamical quantities
Temps, Mags, Susceps, Eints, SpecHeats = myAlloy.MCSimulation(\n
    Tmin=0.05, Tmax=8.\n
    →5, points=40, MCSTEPS=15000, SPARE_MCSTEPS=5000)

```

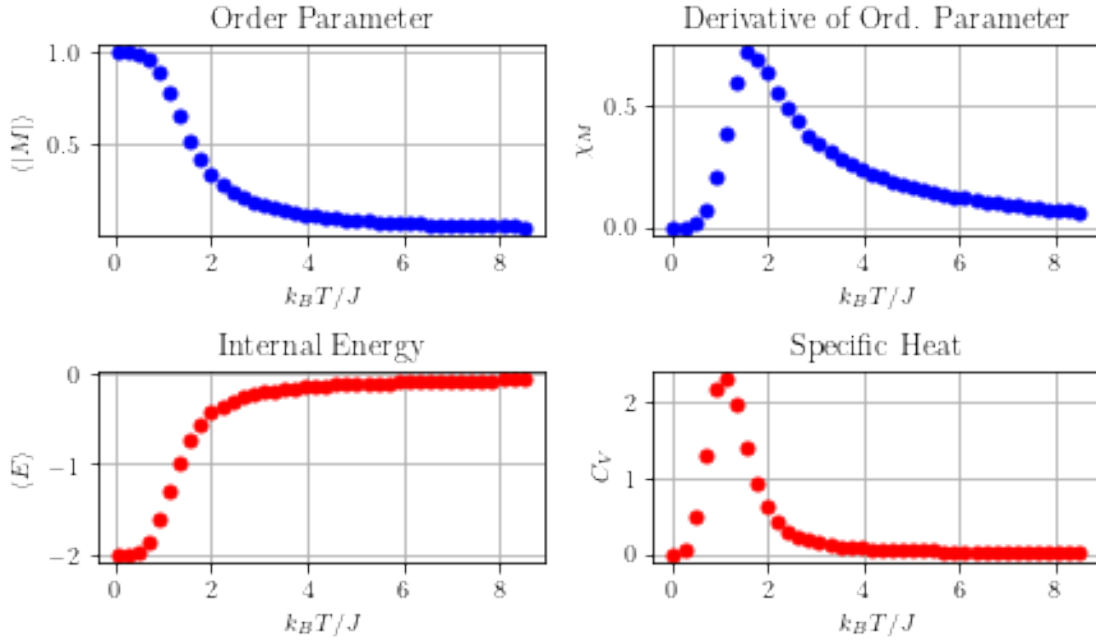
[130]: # Plot results

```

results, quantities = \
plt.subplots(2, 2, constrained_layout = True)
quantities[0,0].plot(Temps,Mags,'bo')
quantities[0,0].set_xlabel(r"$k_BT/J$")
quantities[0,0].set_ylabel(r"$\langle M \rangle$")
quantities[0,0].set_title(r'Order Parameter')
quantities[1,0].plot(Temps,Eints,'ro')
quantities[1,0].set_xlabel(r"$k_BT/J$")
quantities[1,0].set_ylabel(r"$\langle E \rangle$")
quantities[1,0].set_title('Internal Energy')
quantities[1,1].plot(Temps,SpecHeats,'ro')
quantities[1,1].set_xlabel(r"$k_BT/J$")
quantities[1,1].set_ylabel(r"$C_V$")
quantities[1,1].set_title(r'Specific Heat')
quantities[0,1].plot(Temps,Susceps,'bo')
quantities[0,1].set_xlabel(r"$k_BT/J$")
quantities[0,1].set_ylabel(r"$\chi_M$")
quantities[0,1].set_title(r'Derivative of Ord. Parameter')
results.suptitle(\n
    r'\textbf{Binary Alloy Thermodynamic Quantites - MCMC Simulation}'+ '\n' +\n
    r'$\mu = $ '+str(Mukey[int(Muidx)])+r', $h = $ '+str(hkey[int(hidx)]))\n
if save_:\n
    plt.savefig('Figures/ThermalQuantites'+Muidx+'_'+hidx+'.pdf')\n
plt.show()

```

**Binary Alloy Thermodynamic Quantities - MCMC Simulation**  
 $\mu = 0.0, h = 0.5$



Notice that the derivatives of thermodynamic quantities of a stoichiometric alloy present a very sharp peak at the critical temperature  $T_c$  computed before, whereas non-stoichiometric alloys do not present such a sharp peak.

## References

- [1] B. K. Aycan Ozkan. An introduction to the ising model. *International Journ of Modern Physics C*, 20(10):1617 – 1632, 2009.
- [2] S. M. Bhattacharjee and A. Khare. Fifty years of the exact solution of the two-dimensional ising model by onsager. *Current Science*, 69(10):816–821, 1995.
- [3] K. Binder. Kinetic ising model study of phase separation in binary alloys. *Zeitschrift für Physik*, 267:313–322, 1974.
- [4] M. Blume, V. J. Emery, and R. B. Griffiths. Ising model for the lambda transition and phase separation in he3-he4 mixtures. *Physical Review A*, 4(3):1071 – 1078, 1971.
- [5] B. A. Cipra. An introduction to the ising model. *The American Mathematical Monthly*, 94:937 – 959, 1987.
- [6] M. Y. S. David A. Porter, Kenneth E. Easterling. *Phase Transformations in Metals and Alloys*. CRC Press, 3 edition, 2009.
- [7] A. P. Eduard Vives. Kinetics of a vacancy-driven order-disorder transition in a two-dimensional binary alloy. *Physical Review Letters*, 68(6):812 – 815, 1992.
- [8] C. Hoede and H. Zandvliet. *On the solution, the critical exponents and the transition equation of the simple cubic three-dimensional Ising model*. Number Supplement/1878. University of Twente, Department of Applied Mathematics, 9 2008.
- [9] C. Hoede and H. Zandvliet. On the solution, the critical exponents and the transition equation of the simple cubic three-dimensional ising model. *Journal of Micromechanics and Microengineering - J MICROMECHANIC MICROENGINEER*, 01 2008.
- [10] H. L. Hong, Q. Wang, C. Dong, and P. K. Liaw. Understanding the cu-zn brass alloys using a short-range-order cluster model: significance of specific compositions of industrial alloys. *Scientific Reports*, 4(1):7065, 2014.
- [11] T. Horiguchi. A spin-one ising model on a honeycomb lattice. *Physics Letters*, 113A(8):425 – 429, 1986.
- [12] E. Ibarra-García-Padilla, C. G. Malanche-Flores, and F. J. Poveda-Cuevas. The hobbyhorse of magnetic systems: the ising model. *European Journal of Physics*, 37(065103):1 – 27, 2016.
- [13] G. J.D. and D. M. *Introduction to the Theory of Metastable and Unstable States. Lecture Notes in Physics*, volume 183, chapter A Simple model For Binary Alloys, pages 14 – 34. Springer, 1983.
- [14] F. Kos, D. Poland, D. Simmons-Duffin, and A. Vichi. Precision islands in the ising and o(n ) models. *Journal of High Energy Physics*, 2016(8), Aug 2016.
- [15] W. Krauth. *Statistical Mechanics: Algorithms and Computations*. Oxford University Press, 1 edition, 2006.

- [16] P. K. Kumar and L. Muldawer.  $\beta$ -brass critical temperatures and exponents as a function of composition. *Phys. Rev. B*, 14:1972–1976, Sep 1976.
- [17] L. D. Landau and E. M. Lifshitz. *Statistical Physics*, volume 1. Pergamon Press, 3 edition, 1976.
- [18] A. Madsen, J. Als-Nielsen, J. Hallmann, T. Roth, and W. Lu. Critical behavior of the order-disorder phase transition in  $\beta$ -brass investigated by x-ray scattering. *Phys. Rev. B*, 94:014111, Jul 2016.
- [19] E. V. Marcel Porta, Carlos Frontera and T. Castan. Effect of vacancy interaction on antiphase domain growth in a two-dimensional binary alloy. *Physical Review B*, 56(9):5261 – 5270, 1997.
- [20] G. F. Newell and E. W. Montroll. On the theory of the ising model of ferromagnetism. *Rev. Mod. Phys.*, 25:353–389, Apr 1953.
- [21] G. M. M. P. A. Flinn. Monte carlo calculation of the order-disorder transformation in the body-centered cubic lattice. *Physical Review B*, 124(1):54 – 59, 1961.
- [22] M. Porta and T. Castán. Statisticothermodynamic properties of a binary alloy. *American Journal of Physics*, 63:261–267, 1995.
- [23] A. L. Talapov and H. W. J. Blöte. The magnetization of the 3d ising model. *Journal of Physics A: Mathematical and General*, 29(17):5727–5733, sep 1996.
- [24] Y.-L. Wang and C. Wentworth. Phase diagrams of three - dimensional blume - emery - griffiths model. *Journal of Applied Physics*, 61:4411 – 4412, 1987.
- [25] J. M. Yeomans. *Statistical Mechanics of Phase Transitions*. Oxford University Press, 1 edition, 1992.